

# GP38 as a Vaccine Target for Crimean-Congo Hemorrhagic Fever Virus

Matthias Schnell (✉ [matthias.schnell@jefferson.edu](mailto:matthias.schnell@jefferson.edu))

Thomas Jefferson University <https://orcid.org/0000-0001-9040-9405>

Gabrielle Scher

Thomas Jefferson University <https://orcid.org/0000-0002-7571-4791>

Dennis Bente

University of Texas Medical BRanch <https://orcid.org/0000-0002-5150-7368>

Megan Mears

University of Texas Medical Branch

Maria Cajimat

University of Texas Medical Branch

---

## Article

**Keywords:** Crimean-Congo Hemorrhagic Fever Virus, Vaccine, Rabies virus, Vesicular Stomatitis Virus, GP38

**Posted Date:** August 1st, 2022

**DOI:** <https://doi.org/10.21203/rs.3.rs-1882445/v1>

**License:**   This work is licensed under a Creative Commons Attribution 4.0 International License.

[Read Full License](#)

---

1 **GP38 as a Vaccine Target for Crimean-Congo Hemorrhagic Fever Virus**

2 **Gabrielle Scher<sup>1</sup>, Dennis A. Bente<sup>2</sup>, Megan C. Mears<sup>3</sup>, Maria N.B. Cajimat<sup>2</sup>, Matthias J.**  
3 **Schnell<sup>1,4\*</sup>**

4 <sup>1</sup> Department of Microbiology and Immunology, Sidney Kimmel Medical College at Thomas Jefferson  
5 University, Philadelphia, Pennsylvania

6 <sup>2</sup> Galveston National Laboratory, Department of Microbiology and Immunology, Institute for Human  
7 Infections and Immunity, University of Texas Medical Branch, Galveston, Texas, USA.

8 <sup>3</sup> Department of Pathology, University of Texas Medical Branch, Galveston, Texas, USA.

9 <sup>4</sup> Jefferson Vaccine Center, Sidney Kimmel Medical College, Thomas Jefferson University, Philadelphia,  
10 Pennsylvania

11 \* Corresponding authors. Email: [Matthias.Schnell@jefferson.edu](mailto:Matthias.Schnell@jefferson.edu)

13 **Abstract**

14 Crimean-Congo Hemorrhagic Fever Virus (CCHFV) is a tick-borne virus that causes severe  
15 hemorrhagic disease in humans. There is a great need for effective vaccines and therapeutics  
16 against CCHFV for humans, as none are currently internationally approved. Recently, a  
17 monoclonal antibody against the GP38 glycoprotein protected mice against lethal CCHFV  
18 challenge. To show that GP38 is required and sufficient for protection against CCHFV, we used  
19 three inactivated rhabdoviral-based CCHFV-M vaccines, with or without GP38 in the presence  
20 or absence of the other CCHFV glycoproteins. All three vaccines elicited strong antibody  
21 responses against the respective CCHFV glycoproteins. However, only vaccines containing  
22 GP38 showed protection against CCHFV challenge in mice; vaccines without GP38 were not  
23 protective. The results of this study establish the need for GP38 in vaccines targeting CCHFV-M  
24 and demonstrate the efficacy of a CCHFV vaccine candidate based on an established vector  
25 platform.

27 **Key Words:** Crimean-Congo Hemorrhagic Fever Virus; Vaccine; Rabies virus; Vesicular  
28 Stomatitis Virus; GP38

## 29 Introduction

30 Crimean-Congo Hemorrhagic Fever Virus (CCHFV) is an emerging infectious disease with an  
31 extensive global distribution spanning across areas of Africa, Asia, the Middle East, and  
32 Europe<sup>1-5</sup>. The wide range of endemic areas is due to the natural habitat of CCHFV's tick vector,  
33 ticks of the *Hyalomma* genus<sup>1-5</sup>. Areas where this tick can survive are increasing due to  
34 anthropogenic factors such as habitat modification, thus increasing the areas where CCHFV  
35 can circulate<sup>6,7</sup>. CCHFV infects a wide range of mammalian hosts, yet it does not cause visible  
36 disease in these animals<sup>1-5</sup>. However, CCHFV can cause Crimean-Congo hemorrhagic fever  
37 (CCHF) in humans, which first presents with flu-like symptoms and progresses to bleeding,  
38 petechiae, and, in more severe cases, organ failure and death<sup>1-5</sup>. The case-fatality rate for  
39 CCHF is up to 40%<sup>1-5</sup>, and there are no licensed CCHFV-specific vaccines or treatments  
40 available for humans. Therefore, CCHFV is designated as a biosafety level 4 (BSL-4) pathogen,  
41 further highlighting the need for effective vaccines and therapeutics. Accordingly, CCHFV is  
42 classified as an NIH/NIAID Category A and World Health Organization (WHO) high-priority  
43 pathogen.

44 There have been a variety of vaccine strategies against CCHFV tested in animal models with  
45 varying success<sup>8-10</sup>. The only vaccine ever tested in humans was a whole inactivated virus  
46 vaccine propagated in mouse brains that reduced cases in Bulgaria, but requires BSL-4  
47 laboratories for production and is administered as a four dose regimen<sup>11</sup>. While many other  
48 strategies have proven to be protective in animal models<sup>8-10</sup>, there are concerns regarding the  
49 clinical application of each candidate. A cell culture produced whole inactivated virus vaccine  
50 showed 80% protection in mice<sup>12</sup>; however, it requires a BSL-4 facility for production, which is  
51 dangerous and expensive. DNA vaccines using both the nucleoprotein (S) and glycoprotein (M)  
52 genes, individual glycoproteins (G<sub>N</sub> and G<sub>C</sub>) or a combination of these antigens have  
53 demonstrated 100% protection in mice or *Cynomolgus macaques*<sup>13-16</sup>, but DNA vaccines have

54 not been effective in humans. A nucleoside-modified mRNA vaccine using CCHFV  
55 nucleoprotein and/or glycoproteins ( $G_N$  and  $G_C$ ) also showed 100% protection in mice<sup>10</sup>.  
56 However, the study did not investigate the longevity of the immune responses elicited by the  
57 vaccine, which might be a problem based on the findings of waning humoral immune response  
58 to the Severe Acute Respiratory Syndrome Coronavirus 2 (SARS-CoV-2) mRNA vaccine.  
59 Finally, both live Modified Vaccinia Ankara (MVA) and Vesicular Stomatitis virus (VSV) vaccines  
60 containing the CCHFV-M gene protected mice from CCHFV challenge<sup>9,17</sup>, but supporting clinical  
61 studies are pending. While live vaccine strategies can be effective, there is always a concern  
62 about the virulence (whether inherent or mutation acquired) of these vectors, especially when  
63 used in immunocompromised people, pregnant women, and children. Thus, there is still a great  
64 need for an effective and safe CCHFV vaccine strategy.

65 Rhabdoviruses, specifically rabies virus (RABV) and VSV, have been used as vaccine vectors  
66 for a variety of infectious diseases<sup>18</sup>, including CCHFV, as mentioned above<sup>9</sup>. These vectors  
67 have many advantages, including their small, easily manipulated genome that can stably  
68 express foreign glycoproteins<sup>19,20</sup> and their well-established safety profiles<sup>21-25</sup>. Both vectors can  
69 be used as inactivated vaccines that will elicit immune responses against both foreign  
70 glycoproteins and the native rhabdoviral glycoproteins<sup>21-24</sup>; however, VSV has never been tested  
71 as a killed vector. The RABV vaccine has been shown to elicit long-lasting immunity in  
72 humans<sup>26</sup>, which is important for a vaccine platform. Moreover, a rabies-based vaccine against  
73 SARS-CoV-2 is currently being evaluated in humans<sup>27</sup>. Finally, RABV and CCHFV share many  
74 endemic regions, and thus a bivalent vaccine against both viruses would have a significant  
75 impact in the affected areas.

76 CCHFV is a member of the order *Bunyavirales*, family *Nairoviridae*, a group of single-stranded  
77 negative-sense RNA viruses with tri-segmented genomes. Vaccine strategies targeting the  
78 CCHFV M segment have shown protection in mouse challenge models as previously

79 stated<sup>9,10,13,17</sup>. This gene encodes for the virus's glycoproteins, specifically structural proteins G<sub>N</sub>  
80 and G<sub>C</sub>, secreted GP38, and non-structural proteins NS<sub>M</sub> and a mucin-like domain (MLD)<sup>28</sup>. G<sub>N</sub>  
81 and G<sub>C</sub> are embedded in the membrane that encompasses the virion and mediate cell  
82 attachment and entry<sup>28</sup>, and G<sub>N</sub> is suspected of playing a role in virion assembly<sup>29</sup>. GP38 and  
83 the MLD, referred to as GP85, have been shown to play a role in the processing and trafficking  
84 of the structural glycoproteins and are indispensable for viral replication<sup>30</sup>. NS<sub>M</sub> was shown to  
85 play a role in G<sub>C</sub> processing but was not required for viral replication<sup>30</sup>.

86 Currently, there are no defined correlates of protection for CCHFV. Studies using either part of  
87 or the full-length CCHFV-M gene as a vaccine target have shown varying results regarding the  
88 vaccine's protective efficacy<sup>8-10</sup>. Specifically, vaccines that induce immune responses against  
89 the full-length CCHFV-M are protective<sup>9,17,31</sup>, while those that only target the structural proteins  
90 are not protective against CCHFV<sup>13,32</sup>. The humoral immune response elicited during natural  
91 infection is specific for G<sub>C</sub> and GP38<sup>33</sup>. Interestingly, although the G<sub>C</sub> antibodies are neutralizing,  
92 they are not protective, while the GP38 antibodies are non-neutralizing and protective<sup>33,34</sup>.  
93 Additionally, a CCHFV-M based DNA vaccine study showed that GP38 was required for  
94 protection<sup>15</sup>. Thus, GP38 is a very attractive target antigen for a CCHFV vaccine that has not  
95 been extensively tested in the absence of other CCHFV glycoproteins.

96 Here, we present a novel approach to an effective CCHFV vaccine based on RABV virions  
97 containing membrane-anchored GP38. To demonstrate the requirement of immune responses  
98 against GP38 for protection against CCHFV, we have developed two VSV-based inactivated  
99 CCHFV vaccines containing the full M segment with or without GP38. Efficacy of the novel  
100 vaccine was shown in two animal models, a non-BSL-4 VSV-based surrogate challenge model  
101 for CCHFV and challenge with CCHFV in transiently immune suppressed C57BL/6 mice. Our  
102 results indicate that immune responses against GP38 are required for protection against  
103 CCHFV and that the GP85 vaccine is an excellent candidate for a CCHFV vaccine.

104 **Results**

105 *Vaccine Design*

106 To construct the rhabdoviral-based CCHFV vaccines, we used the rabies vector BNSP333 and  
107 VSV vector cVSV-XN. BNSP333 is a well-characterized vector derived from RABV vaccine  
108 strain SAD-B19. SAD-B19 has been further attenuated through an arginine to glutamic acid  
109 mutation at amino acid 333 of the glycoprotein (G) gene, which reduces the vector's  
110 neurotropism<sup>35</sup> and has been used for multiple vaccine approaches (for review see<sup>18</sup>). cVSV-XN  
111 is based on the Indiana strain of VSV<sup>36</sup>, which is attenuated by an unknown mechanism. A  
112 human-codon optimized CCHFV-M (coM) gene from strain IbAr10200 was used as the antigen  
113 for these vaccines<sup>31</sup>. Three different CCHFV vaccines were constructed with an emphasis on  
114 GP38, which we hypothesize is required for a protective CCHFV vaccine (**Figure 1**). BNSP333-  
115 GP85 (GP38+ G<sub>C</sub>-) contains a modified GP85, where CCHFV GP38 is anchored in the RABV  
116 virion by the addition of 51 amino acids of the RABV glycoprotein (G) ectodomain (ED), the  
117 transmembrane domain (TM) and cytoplasmic tail (CT), as used previously to successfully  
118 incorporate other proteins into RABV virions<sup>37-40</sup>. Since the CCHFV MLD is cleaved and  
119 secreted during glycoprotein maturation<sup>41</sup>, the GP38 part is the only protein from CCHFV M  
120 present in this vaccine (**Figure 2e**). The second construct, VSV-ΔG-CCHFV-coM-RVG (GP38-  
121 G<sub>C</sub>+), is a VSV-vectored vaccine containing the full M gene with the terminal 50 amino acids in  
122 the G<sub>C</sub> cytoplasmic tail truncated to allow the glycoproteins to traffic to the plasma membrane<sup>42</sup>  
123 and RABV-G with the 333 attenuating mutation replacing VSV-G. CCHFV M gene expressed by  
124 this vector does not contain GP38 in its virion because GP38 is cleaved from G<sub>N</sub> and secreted  
125 from the cell<sup>41,43</sup>; thus, this vaccine is a negative control for the role of GP38-mediated  
126 protection. Lastly, VSV-ΔG-CCHFV-coM (GP38+ G<sub>C</sub>+), contains the same modified version of  
127 the M gene as GP38- G<sub>C</sub>+ but lacks its own VSV glycoprotein and incorporates GP38 into the

128 virion due to a mutation in the cleavage site between GP38 and G<sub>N</sub> as described previously<sup>9</sup>.

129 Therefore, the GP38+ G<sub>C</sub>+ vaccine is a positive control for GP38-mediated protection.

130 All viruses were recovered, passaged twice and sequenced. The GP38+ G<sub>C</sub>+ virus developed

131 two mutations, L517R and L518S, in the cleavage motif between GP38 and G<sub>N</sub>, as mentioned

132 above, and the GP38+ G<sub>C</sub>- and GP38- G<sub>C</sub>+ viruses did not acquire any mutations.

### 133 *Incorporation of CCHFV Glycoproteins into Rhabdoviral Vectors*

134 To assess the expression of the CCHFV genes in the rhabdoviral vectors, we did

135 immunofluorescence (IF) surface staining and flow cytometry analysis of VeroE6 cells infected

136 with each virus. For IF, cells were infected at a multiplicity of infection (MOI) of 0.01. RABV

137 infected cells were incubated for 72hrs, and VSV infected cells were incubated for 24hrs. For

138 flow cytometry, VeroE6 cells were infected at MOI 10 for RABVs and MOI 5 for VSVs and

139 incubated for 48hrs or 8hrs respectively. After infection, cells were fixed and stained with anti-

140 RABV-G human monoclonal antibody 4C12 and either anti-CCHFV-Gc antibody 11E7 or anti-

141 CCHFV-GP38 antibody 13G8. Surface staining of the infected cells showed that all the CCHFV

142 proteins present in each of the rhabdoviruses were present on the cell surface (**Figure 2a-d,**

143 **S1**). RABV-G was detected from all the RABV-based vectors tested and the GP38- G<sub>C</sub>+ virus

144 which was engineered to contain RABV-G (**Figure 2a-d, S1**).

145 To analyze the incorporation of the glycoproteins, we sucrose purified virions and separated the

146 proteins on SDS Page protein gels. SYPRO™ Ruby staining showed incorporation of all the

147 native rhabdoviral proteins in each virus (**Figure 2e, S2a,b**). Western blotting for GP38 and Gc

148 demonstrated that only GP38+ G<sub>C</sub>- and GP38+ G<sub>C</sub>+ viruses incorporate GP38, whereas GP38+

149 G<sub>C</sub>+ and GP38- G<sub>C</sub>+ viruses incorporate Gc (**Figure 2f, S2c**). RABV-G was detected for the

150 GP38- G<sub>C</sub>+ virus (**Figure 2f, S2c**).

151 To analyze virus growth kinetics, we performed multi- and one-step growth curves for RABVs  
152 and one-step growth curves for VSVs. For multi-step growth curves, cells were infected at a low  
153 MOI of 0.01, and for one-step growth curves, cells were infected at a high MOI of 10. All CCHFV  
154 vaccine viruses showed slower growth kinetics compared to their parental vectors (**Figure 2g-i**).  
155 Regardless of kinetics, all viruses grew to sufficient titers of at least  $1 \times 10^6$  focus forming units  
156 (ffu) for RABVs or plaque forming units (pfu) for VSVs.

157 These results show that rhabdoviruses with CCHFV glycoprotein genes are recoverable and  
158 incorporate the expected proteins into the virions.

#### 159 *The Mucin-Like Domain Is Required for GP38 Expression*

160 We previously designed a vaccine that had GP38 with the RABV-G tail anchor but without the  
161 MLD, called BNSP333-GP38 (**Figure S3a**). This virus was recovered, and characterization  
162 showed very poor expression of GP38. Immunofluorescence staining for GP38 on cells infected  
163 with BNSP333-GP85 showed very strong surface and intracellular expression of GP38, while  
164 cells infected with BNSP333-GP38 showed very minimal GP38 expression (**Figure S3b**). Flow  
165 cytometry analysis of cells infected with BNSP333-GP38 or BNSP333-GP85 showed  
166 comparable levels of RABV-G expression between viruses, but only BNSP333-GP85 had high  
167 levels of GP38 (**Figure S3c**). Finally, western blot for GP38 of sucrose purified virions showed  
168 that BNSP333-GP38 has virtually no incorporation of GP38 into virions compared to BNSP333-  
169 GP85 (**Figure S3d**). These data show that the MLD is required for proper expression and  
170 incorporation of GP38 into rhabdoviruses.

#### 171 *Immunogenicity of Rhabdoviral-based CCHFV Vaccines*

172 To investigate the immunogenicity of the vaccines, we immunized groups of 5 C57BL/6 (B6)  
173 mice with two doses, 28 days apart, of  $10 \mu\text{g}$  of  $\beta$ -propiolactone inactivated vaccines (**Figure**  
174 **3a,b**). We used two groups per vaccine, one immunized with deactivated vaccine alone, the



175 other containing deactivated vaccine adjuvanted with 5µg of TLR-4 agonist synthetic  
176 Monophosphoryl Lipid A (MPLA), 3D(6A)-PHAD (PHAD), in a 2% squalene-in-oil emulsion (SE).  
177 The mice were bled at various time points (**Figure 3a**). All mice developed antibody responses  
178 against their respective antigens by day 14 post-immunization, which increased after the boost  
179 on day 28 and were maintained out to day 56 (**Figure 3**). Using an adjuvant during vaccination  
180 typically improves the immune responses elicited by the vaccine<sup>44-46</sup>. Adjuvanted groups  
181 showed higher antibody responses for all vaccines against their respective antigens (**Shown for**  
182 **GP38, Figure S4**). Thus, we decided to use adjuvants for all subsequent studies.

### 183 *Rhabdoviral-based CCHFV Vaccines Elicit a Th1-biased Antibody Response*

184 Th1 immune responses have been associated with strong anti-viral responses<sup>47-50</sup>. In B6 mice,  
185 IgG2b and IgG2c are associated with Th1 responses, while IgG1 is associated with Th2  
186 responses<sup>51</sup>. We performed isotype subclass ELISAs using the day 56 sera from the  
187 immunogenicity study. All vaccines showed strong IgG2c and IgG2b antibody responses for  
188 their respective antigens, indicating a skew towards a Th1-associated response (**Figure 4**).

### 189 *A VSV-based Surrogate Challenge Model as a Tool for Determining CCHFV Vaccine Efficacy.*

190 CCHFV is a BSL-4 pathogen, which makes animal experiments with CCHFV expensive.  
191 Therefore, we developed a VSV-based surrogate challenge model for CCHFV. Pilot studies  
192 revealed that in IFNAR<sup>-/-</sup> mice, this virus consistently causes high viremia and modest disease  
193 regardless of challenge dose (**data not shown**).

194 To test the utility of this challenge model for initial screening of vaccine efficacy, we immunized  
195 groups of male and female IFNAR<sup>-/-</sup> mice with either GP38+ Gc- vaccine or control FR1 vaccine,  
196 both adjuvanted with PHAD-SE (**Figure 5a,b**). We included a naïve B6 group as a control for  
197 protection since these mice are not susceptible to this virus (**Figure 5b**). All IFNAR<sup>-/-</sup> mice

198 immunized with the GP38+ G<sub>C</sub>- vaccine developed antibodies against CCHFV GP38, but we  
199 observed gender differences in antibody titer (**Figure 5c**).

200 On day 65 post immunization, the vaccinated IFNAR<sup>-/-</sup> and naïve B6 mice were challenged  
201 intraperitoneally (I.P.) with 5E5pfu of the surrogate challenge virus (GP38+ G<sub>C</sub>+). Mice  
202 immunized with the GP38+ G<sub>C</sub>- vaccine showed minimal weight fluctuation post-challenge,  
203 while mice immunized with the FR1 vaccine showed modest weight loss (**Figure 5d, S5**). One  
204 female and one male mouse from the FR1 immunized groups met endpoint euthanasia criteria  
205 on day 5 post-challenge. Mice vaccinated with the FR1 vaccine showed high viral RNA copies in  
206 the blood at 4 days post-infection, which were 3-5-fold higher compared to mice immunized with  
207 the GP38+ G<sub>C</sub>- vaccine, with some females completely clearing the virus (**Figure 5e**). Mice  
208 vaccinated with the GP38+ G<sub>C</sub>- had a boost in GP38-specific antibody titers post-challenge  
209 (**Figure 5f**).

210 These data show that the VSV-based surrogate challenge model for CCHFV can be used to test  
211 vaccine efficacy under BSL-2 conditions.

#### 212 *Rhabdoviral-based CCHFV Vaccine Efficacy Against Wildtype CCHFV Challenge*

213 To determine the protective efficacy of these rhabdoviral-based CCHFV vaccines, we performed  
214 a challenge experiment with wildtype (WT) CCHFV. B6 mice were immunized with 10µg of  
215 vaccine/dose adjuvanted with PHAD-SE following the same prime/boost schedule used above  
216 for the immunogenicity studies (**Figure 6a**). For this study, we utilized two groups of 5 mice per  
217 vaccine, one female and the other male, to detect any differences between the sexes. ELISAs  
218 against GP38 and G<sub>C</sub> with sera collected at day 35 showed that all vaccines elicited strong  
219 antibody responses against the expressed CCHFV antigens, and there were no differences in  
220 antibody titers between sexes in the B6 mice (**Figure S6**).

221 Given that WT mice are resistant to CCHFV infection, the immunized B6 mice were treated with  
222 anti-interferon  $\alpha/\beta$  receptor 1 (IFNAR) monoclonal antibody mAb-5A3 to make them susceptible  
223 and then challenged I.P. with 1000pfu of CCHFV, strain IbAr10200. Mice vaccinated with either  
224 the GP38+ G<sub>C</sub><sup>-</sup> or GP38+ G<sub>C</sub><sup>+</sup> vaccines maintained weight throughout the course of the  
225 challenge, while mice vaccinated with GP38- G<sub>C</sub><sup>+</sup>, FR1, or PBS showed dramatic weight loss  
226 starting by day 3 post challenge (**Figure 6c**). All mice vaccinated with either GP38+ G<sub>C</sub><sup>-</sup> or  
227 GP38+ G<sub>C</sub><sup>+</sup> vaccines survived challenge out to day 21 and did not show any outward clinical  
228 signs of disease (**Figure 6d, S7**). However, all mice vaccinated with either GP38- G<sub>C</sub><sup>+</sup>, FR1 or  
229 PBS succumbed to disease, with most mice reaching endpoint euthanasia criteria between days  
230 4-6, except for one male mouse vaccinated with FR1 (**Figure 6d**). There were no significant  
231 differences in weight loss or survival between mice of different sexes immunized with the same  
232 vaccine.

233 These results confirmed that only mice receiving vaccines containing GP38 (i.e., GP38+ G<sub>C</sub><sup>-</sup>  
234 and GP38+ G<sub>C</sub><sup>+</sup>) were protected against lethal CCHFV challenge.

#### 235 *Vaccine-Induced Virus Neutralization Does Not Correlate with Protection*

236 To determine the CCHFV neutralizing capabilities of the rhabdoviral-based CCHFV vaccines,  
237 we performed a focus reduction neutralization test (FRNT) using a recombinant CCHFV  
238 expressing ZsGreen. Previous studies have suggested that protection from lethal challenge is  
239 achieved with neutralizing antibody titers of 1:160<sup>9,12,13,31,32</sup>, which in this assay, corresponds to  
240 100% virus neutralization when using the hyper-immune mouse ascitic fluid (HMAF) control.  
241 The GP38+ G<sub>C</sub><sup>+</sup> vaccine had a FRNT<sub>50</sub> of <1:1280 and showed neutralizing activity comparable  
242 to HMAF, with 100% virus neutralization at a 1:160 serum dilution (**Figure 7a**). The GP38+ G<sub>C</sub><sup>-</sup>  
243 and GP38- G<sub>C</sub><sup>+</sup> vaccines demonstrated minimal neutralization at a 1:160 serum dilution, similar  
244 to FR1 immunized control mice (**Figure 7a**). These data indicate that vaccine-induced  
245 neutralizing antibodies are not the mechanism of protection for these vaccines.

246 We also analyzed a virus neutralization assay (VNA) for RABV. For RABV, induction of high  
247 levels of neutralizing antibodies post-vaccination correlates with protection<sup>52</sup>. As measured  
248 through the rapid fluorescent focus inhibition assay (RFFIT), mice immunized with GP38+ G<sub>C</sub><sup>-</sup>,  
249 GP38- G<sub>C</sub><sup>+</sup>, or FR1 vaccines all showed high levels of RABV neutralizing antibodies, well above  
250 the 0.5 international units (IU)/mL threshold considered protective by the WHO (**Figure 7b**). No  
251 RABV-neutralization was observed in mice immunized with the GP38+ G<sub>C</sub><sup>+</sup> vaccine (**Figure**  
252 **7b**).

253

254

255 **Discussion**

256 CCHFV is an emerging disease for which no licensed treatments or vaccines are available. To  
257 this end, we developed an inactivated RABV-vectored CCHFV vaccine targeting the GP38  
258 protein. This killed virus vaccine platform was safe to administer to both WT and  
259 immunocompromised (IFNAR<sup>-/-</sup>) mice and showed protection against lethal challenges in mice.  
260 Although GP38 is unique to the nairoviruses<sup>53</sup>, it has not been widely investigated as a potential  
261 vaccine target. However, it was recently shown that GP38 is indispensable for viral replication<sup>30</sup>  
262 and GP38 targeted immune responses elicited protection against CCHFV challenge<sup>15,34</sup>. Thus,  
263 we decided to tailor our vaccine approach to target GP38.

264 We initially constructed a recombinant RABV containing a chimeric GP38/RABV G gene. This  
265 virus had poor expression and no GP38 incorporation, indicating that the MLD is required for  
266 GP38 processing. There is some evidence in the literature supporting this idea. Deleting of the  
267 MLD changes GP38 localization and affects the incorporation of the structural glycoproteins into  
268 tc-VLPs<sup>30</sup>. However, we believe that we have shown here for the first time with a live viral vector  
269 that the MLD is required for the proper processing of CCHFV GP38.

270 Moreover, we developed a BSL-2 surrogate challenge model to test CCHFV vaccine efficacy,  
271 given the challenges of performing such studies in BSL-4 labs. We previously demonstrated that  
272 such a model using a VSV with its native glycoproteins replaced with the LASV glycoproteins  
273 was useful for determining the mechanism of protection for a RABV-based LASV vaccine<sup>22</sup>.

274 While the CCHFV model was not uniformly lethal in IFNAR<sup>-/-</sup> mice, it did cause consistently high  
275 levels of viremia, an indicator of significant replication in the host. Additionally, we saw that the  
276 GP38+ G<sub>C</sub>- vaccine elicited protection in this surrogate challenge model, demonstrating its utility  
277 in analyzing vaccine protective efficacy. Of note, the results detected in the surrogate model  
278 translated well to the finding in the WT CCHFV challenge further indicating the model's  
279 usefulness.

280 We hypothesized that only CCHFV-M targeting vaccines containing GP38 would be protective  
281 against CCHFV challenge. Our study confirmed the hypothesis that GP38 is required and  
282 sufficient for protection. We saw that both the GP38+ G<sub>C</sub>- and GP38+ G<sub>C</sub>+ vaccines protected  
283 100% of mice against lethal CCHFV challenge, while our control mice, including the GP38- G<sub>C</sub>+  
284 vaccinated mice, all succumbed to challenge. The full-length CCHFV-M gene or individual  
285 components have been tested as a CCHFV vaccine target in many vaccine strategies<sup>8-10,15,31,32</sup>.  
286 In line with our hypothesis that GP38 is required for protection when targeting CCHFV-M,  
287 vaccine strategies that use the entire M gene, such as DNA vaccines<sup>15,16,31</sup> or live viral  
288 vectors<sup>9,17</sup>, have shown protection against WT CCHFV challenge. However, those vaccine  
289 strategies that exclude GP38<sup>13,32</sup> or do not develop immune responses against GP38<sup>54</sup> are not  
290 protective against CCHFV challenge. Thus, we have confirmed that GP38 is an excellent  
291 vaccine target for CCHFV.

292 Our GP38+ G<sub>C</sub>- vaccine was protective against WT CCHFV challenge, with no visible weight  
293 loss or clinical signs. These results are comparable to other vaccine strategies targeting  
294 CCHFV-M that were protective against CCHFV challenge, including a live VSV-vectored  
295 vaccine<sup>9</sup>, live MVA-vectored vaccine<sup>17</sup>, and CCHFV-M DNA vaccine<sup>15</sup>. However, our vaccine  
296 candidate has a few advantages over these other strategies. As mentioned above, our vaccine  
297 is a deactivated virus, making it safe to administer to various immunocompromised populations  
298 and pregnant women, unlike live virus vaccines. Additionally, the DNA vaccine used a three  
299 dose immunization schedule<sup>15</sup>, while ours showed protection after only two doses.

300 Mice immunized with our various CCHFV vaccines showed strong antibody responses against  
301 their respective CCHFV glycoproteins and RABV-G with a skew towards a Th1 response. Two  
302 different CCHFV DNA vaccination strategies have investigated the types of antibody responses  
303 elicited from vaccination and showed that Th1 biased antibody responses were protective  
304 against CCHFV challenge<sup>13,31</sup>. Additionally, one of the studies demonstrated that vaccines

305 eliciting a Th2 biased response were less protective compared to those eliciting a Th1 biased  
306 response<sup>13</sup>. The results of our vaccine study agree with these studies, further indicating that Th1  
307 associated responses elicited by CCHFV vaccines are important for protection.

308 As far as we can tell, we are the only study to investigate whether there are sex differences for  
309 the immune responses elicited by CCHFV vaccines in mice. In B6 mice, there were no  
310 significant differences in the antibody responses elicited by these vaccines between males and  
311 females; however, there were significant differences in antibody titers between sexes in the  
312 IFNAR<sup>-/-</sup> mice. It is well documented that there are differences in vaccine-elicited immune  
313 responses between males and females<sup>55</sup>. However, it is intriguing to see this difference in the  
314 IFNAR<sup>-/-</sup> mice but not the WT mice, indicating the need to analyze a vaccine in different models.  
315 Regardless, our studies indicate this vaccine is effective in mice regardless of sex or immune  
316 status, something that is very important for an ideal vaccine candidate.

317 The correlates of protection for CCHFV are still unclear. For many viruses, including RABV<sup>52</sup>,  
318 neutralizing antibodies are considered the correlate of protection against viral infection. For  
319 CCHFV, this does not seem to be the case, as vaccines eliciting high levels of neutralizing  
320 antibodies or treatment with neutralizing mAbs were not protective against CCHFV challenge<sup>32-  
321 34</sup>. Additionally, antibodies against GP38, which thus far have only been shown to have non-  
322 neutralizing functions, elicit protection against CCHFV challenge<sup>33,34</sup>. We also saw this in our  
323 study, with the GP38+ G<sub>C</sub>- vaccine eliciting an antibody response with minimal neutralizing  
324 activity but 100% protection of mice against WT CCHFV challenge. This provides further  
325 evidence that neutralizing antibodies are not a requirement for vaccine-mediated protection  
326 against CCHFV.

327 Given the success of our GP38+ G<sub>C</sub>- vaccine in this study, future testing is warranted to further  
328 characterize this vaccine and determine its utility in other preclinical models. This study focused  
329 on humoral immune responses to investigate the antigenic requirements for CCHFV vaccine-

330 elicited protection, thus cellular responses were outside the scope of the study. However,  
331 various groups have shown that CCHFV vaccine strategies induce CCHFV-specific T cell  
332 responses<sup>10,15,17</sup>. Thus, determining the T cell epitopes targeted by our vaccine is a logical next  
333 step. The only study to investigate CCHFV vaccine mechanisms of protection showed that a live  
334 MVA-vectored CCHFV-M vaccine required both humoral and cellular responses for protection<sup>56</sup>.  
335 A similar study investigating the protective effects of passive and/or adoptive transfer from mice  
336 immunized with our vaccine would be integral to understanding how our vaccine protects.  
337 Additionally, we saw that our GP38+ G<sub>C</sub>- vaccine had minimal CCHFV neutralization, thus it  
338 would be beneficial to investigate non-neutralizing antibody functions in combination with the  
339 passive transfer studies. Finally, testing the efficacy of our vaccine in the fully  
340 immunocompetent non-human primate (NHP) model<sup>57</sup> is essential for confirming the vaccine's  
341 efficacy and advancing this vaccine candidate to clinical trials.

342 In summary, this study shows that for CCHFV-M vaccines, GP38 is required and sufficient for  
343 protection. The GP38+ G<sub>C</sub>- (BNSP333-GP85) vaccine can progress to further testing in NHP  
344 and is an excellent candidate to be moved to the clinic.

345

346



347 **Acknowledgements:** This work was supported in part by NIH grant T32AI134646 (Thomas  
348 Jefferson University), by the Jefferson Vaccine Center and internal UTMB funds. We thank Liz  
349 Declan (Thomas Jefferson University, Philadelphia, PA) for critical reading and editing of the  
350 manuscript. We thank Dr. Aura Garrison (United States Army Medical Research Institute of  
351 Infectious Diseases, Fort Detrick, MD) for CCHFV M cDNA and Dr. Éric Bergeron (United  
352 States Centers for Disease Control, Atlanta, GA) for CCHFV-GP38 cDNA and SW-13 cells.

353

### 354 **Author Contributions**

355 Gabrielle Scher: Conceptualization, Formal Analysis, Investigation, Methodology, Visualization,  
356 Writing – original draft

357 Dennis A. Bente: Investigation, Supervision, Funding acquisition, Writing – review & editing

358 Megan C. Mears: Investigation, Writing – review & editing

359 Maria N. B. Cajimat: Investigation

360 Matthias J. Schnell: Conceptualization, Funding acquisition, Project administration, Supervision,  
361 Writing – review & editing

362

### 363 **Declarations of Interests**

364 Gabrielle Scher and Matthias J. Schnell are inventors on the U.S. Patent Application, “A  
365 therapeutic against Crimean-Congo Hemorrhagic Fever virus”.

366

367 **Figure Legends**

368 **Figure 1. Rhabdoviral-based CCHFV vaccine vector maps**

369 Schematics of the RABV- and VSV-based CCHFV vaccines and their vector controls. All foreign  
370 genes were inserted into the BNSP333 vector between N and P and between M and L for the  
371 VSV vector. The GP85 chimeric gene is expanded to show the various sections of both GP85  
372 and the RABV-G that were included in the gene. Attenuating R333E mutation is marked in  
373 RABV-G. N, nucleoprotein; P, Phosphoprotein; M, matrix protein; G, glycoprotein; L,  
374 polymerase; MLD, Mucin-like domain; ED51, 51 amino acids of the ectodomain; TM,  
375 transmembrane domain; CD, cytoplasmic domain.

376 **Figure 2. Rhabdoviral vectors express and incorporate CCHFV glycoproteins**

377 Characterization of rhabdoviral-vectored CCHFV vaccines through Immunofluorescence (A, B),  
378 flow cytometry (C), SDS PAGE protein gel (D), Western Blot (E), and Growth Curves (F). Vero  
379 E6 cells were infected at MOI 0.01 and fixed after 72 or 24hrs for RABVs and VSVs,  
380 respectively. Cells were stained with  $\alpha$ -RABV-G 4C12 (purple) and  $\alpha$ -CCHFV-Gc 11E7 (A) or  $\alpha$ -  
381 CCHFV-GP38 13G8 (B) (red) and mounted with mounting media containing a nuclear DAPI  
382 stain (blue). In the merged images, GFP from VSV GFP is green, and areas where there is  
383 overlapping expression of RABV-G and the CCHFV glycoproteins are pink. Images were taken  
384 at 40X magnification with a 2X zoom. Scale bars represent 10 $\mu$ m. (C) Vero E6 cells were  
385 infected at MOI 10 and fixed after 48hrs for RABVs or infected at MOI 5 and fixed after 8hrs for  
386 VSVs. Cells were probed for  $\alpha$ -RABV-G 4C12 and  $\alpha$ -CCHFV-Gc 11E7 or  $\alpha$ -CCHFV-GP38  
387 13G8 and analyzed by flow cytometry. Assay was performed multiple times, and the graph is  
388 one representative experiment. (D) SDS PAGE protein gel of sucrose purified virions. 1 $\mu$ g of  
389 each virus was loaded onto the gel and all native rhabdoviral proteins and foreign proteins are  
390 indicated by the arrows next to each gel. (E) Western blot of sucrose purified virions. 1 $\mu$ g of  
391 each virus was loaded onto the gel and transferred to a nitrocellulose membrane for western

392 blotting. Blots were either probed with  $\alpha$ -CCHFV-GP38 13G8 (top panel),  $\alpha$ -CCHFV-Gc 11E7  
393 (middle panel) or  $\alpha$ -RABV-G 4C12 (bottom panel). (F) Multi-step and one-step growth curves.  
394 Cells were infected at MOI 0.01 for multi-step or MOI 10 for one-step growth curves and  
395 samples were titered in triplicate. Statistics are differences in titer compared to the parental  
396 vector for each growth curve (\*\*\*\* $P < 0.0001$ ; \*\*\* $P < 0.0002$ ; \*\* $P < 0.0021$ ; \* $P < 0.0332$ ).

397 **Figure 3. Rhabdoviral-based CCHFV vaccines elicit humoral responses against**  
398 **respective antigens**

399 Immunogenicity study to look at antibody responses induced by each CCHFV vaccine. (A)  
400 Immunization and blood draw schedule for mouse studies. Mice were immunized with  
401 10 $\mu$ g/dose of BPL inactivated vaccines adjuvanted with 5 $\mu$ g of PHAD in 2% SE per dose.  
402 Syringes represent immunizations, red blood drops indicate the days blood was taken and the  
403 skull denotes the conclusion of the study when the mice were sacrificed. (B) Table showing the  
404 vaccine groups used in this study and the symbols and colors used to denote each group and  
405 assay controls. (C, E, G) Group average ELISA curves for each adjuvant at the peak of the  
406 antibody response. (D, F, H) EC<sub>50</sub> ELISA titers over time for each antigen. Error bars indicate  
407 the mean with standard deviation (SD) for groups of 5 mice with samples run in duplicate. An  
408 ordinary one-way ANOVA with Tukey's Multiple Comparison Test was used to determine  
409 statistical differences between groups at each time point. All groups with detectable antibody  
410 titers have 4-star significance compared to groups where no antibody titers were detected  
411 (\*\*\*\* $P < 0.0001$ ; \*\*\* $P < 0.0002$ ; \*\* $P < 0.0021$ ; \* $P < 0.0332$ ; ns = not significant). (C, D)  $\alpha$ -CCHFV-  
412 GP38 ELISAs, (E, F)  $\alpha$ -CCHFV-Gc ELISAs, and (G, H)  $\alpha$ -RABV-G ELISAs. ●, mouse 1; ■,  
413 mouse 2; ▲, mouse 3; ▼, mouse 4; ◆, mouse 5.

414 **Figure 4. Rhabdoviral-based CCHFV vaccines induce a Th1-skewed humoral response**

415 Isotype subclass ELISAs for each vaccine that had detectable antibodies in the CCHFV  
416 glycoprotein IgG Fc ELISAs. (A, C) EC<sub>50</sub> antibody titers for each isotype subclass. (B, D) Isotype  
417 ratios comparing EC<sub>50</sub> titers of IgG2c or IgG2b to IgG1. Any animals with undetectable IgG1  
418 were excluded from isotype ratio calculations. (A, B) GP38 isotype subclass ELISAs. (C, D) Gc  
419 isotype subclass ELISAs. Error bars indicate the mean with standard deviation (SD) for groups  
420 of 5 mice with samples run in duplicate. Mann Whitney test was used to determine statistical  
421 differences between groups for each isotype. (\*\*\*\* $P < 0.0001$ ; \*\*\* $P < 0.0002$ ; \*\* $P < 0.0021$ ;  
422 \* $P < 0.0332$ ; ns = not significant).

### 423 **Figure 5. GP38+ Gc- vaccine is protective in VSV-based surrogate challenge model**

424 Challenge study to determine the utility of a VSV-based surrogate challenge virus when looking  
425 at vaccine protective efficacy. (A) Experimental timeline. Groups of 5 mice were immunized with  
426 10µg/dose of BPL inactivated vaccines adjuvated with 5µg of PHAD in 2% SE per dose as  
427 indicated by the syringe with the rhabdovirus containing multiple glycoproteins. Challenge of  
428 5E5pfu of surrogate virus is indicated by the syringe with a VSV with a singular set of  
429 glycoproteins. Red blood drops indicate the days blood was taken, and the skull denotes the  
430 conclusion of the study when any surviving mice were sacrificed. (B) Table of vaccine groups  
431 and representative colors. GP38 EC<sub>50</sub> titers pre-challenge (C) and post-challenge (F). Error bars  
432 indicate the mean with standard deviation (SD) for groups of 5 mice with samples run in  
433 triplicate. (D) Average group weight curves. Error bars indicate SD. (E) Viral RNA copies in the  
434 blood as determined by VSV-N qPCR. Error bars indicate the mean with SD. Results show the  
435 combination of two independent experiments; hollow symbols represent the first experiment and  
436 symbols with a black outline represent the second experiment. An ordinary one-way ANOVA  
437 with Tukey's Multiple Comparison Test was used to determine statistical differences between  
438 groups at each time point for EC<sub>50</sub> titers and viremia (C, E, F). Two-way ANOVA with Tukey's  
439 Multiple Comparison Test was used to determine statistical differences between groups for the

440 weight curves (D). All comparisons between groups not listed on the EC<sub>50</sub> or weight change  
441 graphs had 4-star significant difference. (\*\*\*\* $P < 0.0001$ ; \*\*\* $P < 0.0002$ ; \*\* $P < 0.0021$ ;  
442 \* $P < 0.0332$ ; ns = not significant).

#### 443 **Figure 6. Vaccines that incorporate GP38 are protective against WT CCHFV Challenge**

444 Challenge study to determine rhabdoviral-based CCHFV vaccine protective efficacy against  
445 CCHFV. (A) Experimental timeline. Groups of 5 mice were immunized with 10 $\mu$ g/dose of BPL  
446 inactivated vaccines adjuvanted with 5 $\mu$ g of PHAD in 2% SE per dose as indicated by the  
447 syringe with the rhabdovirus. As denoted by the syringe with the antibody, mice were given mAb  
448 5A3 24hrs before and after challenge to make them susceptible to CCHFV. The syringe with the  
449 CCHFV indicates when mice were challenged with 1000pfu of strain IbAr10200 I.P. Red blood  
450 drops indicate the days blood was taken and the skull denotes the conclusion of the study when  
451 any surviving mice were sacrificed. (B) Table of vaccine groups, the expected outcome for that  
452 group and their representative colors. (C) Group average weight change over time. Error bars  
453 represent standard deviation. Dotted line indicates weight loss threshold for euthanasia.  
454 Statistics are two-way ANOVA compared to female PBS control group (\*\*\*\* $P < 0.0001$ ). (D)  
455 Kaplan-Meyer survival curves. Log-rank Mantel-Cox test was used to determine the significance  
456 of survival of each group compared to the female PBS control group (\*\* $P < 0.0021$ ).

#### 457 **Figure 7. GP38 does not elicit CCHFV neutralizing antibodies**

458 CCHFV and RABV neutralization assays. (A) Focus reduction neutralization test (FRNT) of a  
459 CCHFV strain IbAr10200 expressing ZsGreen (rCCHFV-ZsGreen) with sera from mice  
460 immunized with rhabdoviral vaccines. Hyperimmune mouse ascitic fluid (HMAF) against CCHFV  
461 served as a positive control. Error bars represent standard deviation (SD). (B) Rapid fluorescent  
462 focus inhibition test (RFFIT) with sera from mice immunized with rhabdoviral vaccines against  
463 RABV (strain CVS-11). Graph shows the RABV neutralizing IU/mL values for individual mice.

464 Error bars represent SD. Ordinary one-way ANOVA with Tukey's Multiple Comparison Test was  
465 used to determine statistical differences between groups. All groups with detectable RABV  
466 neutralizing antibody titers have 4-star significance compared to groups where no antibody titers  
467 were detected ( $****P < 0.0001$ ;  $***P < 0.0002$ ;  $**P < 0.0021$ ;  $*P < 0.0332$ ; ns = not significant).  
468 Dotted line indicates 0.5IU/mL, the WHO suggested protective threshold. ●, mouse 1; ■,  
469 mouse 2; ▲, mouse 3; ▼, mouse 4; ◆, mouse 5.

470

471

472

473

474

475

476

477

478 **Data Availability**

479 All data are available upon request to the lead contact author. No proprietary software was used  
480 in the data analysis.

481 **Materials Availability**

482 Upon request, further information, resources, and reagents are available from the authors  
483 pending an executed MTA as well as biosafety approval of the requesting institutions(s).

484 **Methods**

485 *Animals*

486 C57BL/6 mice (Charles River) and B6.129S2-*Ifnar1<sup>tm1Agt</sup>*/Mmjax (The Jackson Laboratory) mice  
487 ages 6-10 weeks were used in this study. Both males and females were used. Mice used in this  
488 study were handled in adherence to the recommendations described in the *Guide for the Care*  
489 *and Use of Laboratory Animals* and the guidelines of the National Institutes of Health, the Office  
490 of Animal Welfare, and the United States Department of Agriculture. All animal protocols were  
491 approved by the Institutional Animal Care and Use Committee (IACUC) of Thomas Jefferson  
492 University (TJU) or University of Texas Medical Branch (UTMB) for experiments performed at  
493 each facility. The facilities where this research was conducted are fully accredited by the  
494 Association for Assessment and Accreditation of Laboratory Animal Care International. Mice  
495 were housed in cages, in groups of 5, under controlled conditions of humidity, temperature, and  
496 light (12hr light/12hr dark cycles). Food and water were available ad libitum. Animal procedures  
497 at TJU were conducted under 3% isoflurane/O<sub>2</sub> gas anesthesia by trained personnel under  
498 supervision of veterinary staff.

499 *Cells*

500 Vero (ATCC® E6™), 293T (available from the Schnell laboratory), BSR (available from the  
501 Schnell laboratory) and BEAS-2B (ATCC® CRL-9609™) cells were cultured using DMEM  
502 (Corning®) with 5% fetal bovine serum (FBS) (Atlanta-Biologicals®) and 1% Penicillin-  
503 Streptomycin (P/S) (Gibco®). 293F (ATCC® CRL-12585™) cells were cultured using

504 FreeStyle™ 293 Expression Medium (Gibco®) with 2X Glutamax (Gibco®). Mouse  
505 neuroblastoma (NA) (available from the Schnell laboratory) cells were cultured using RPMI  
506 (Corning®) with 5% FBS and 1X P/S. Human hepatocarcinoma cells (HuH-7) (available from  
507 the Bente Laboratory) and SW-13 cells (available from the Bente Laboratory) were maintained  
508 in Dulbecco's modified Eagle's medium (DMEM) supplemented with 10% FBS (Invitrogen,  
509 Carlsbad, CA), 2mM L-glutamine (Invitrogen), and 1% P/S (Invitrogen), cumulatively called D10.  
510 All cells except 293F were stored in incubators with 5% CO<sub>2</sub> at 37°C for normal cell culture or  
511 34°C for virus infected cells. 293F cells were stored in incubators with 8% CO<sub>2</sub> at 37°C and  
512 shaking at 140 rpm.

### 513 *Viruses*

514 RABV strain CVS-11 was produced in our laboratory on NA cells and is available upon  
515 request. A recombinant CCHFV, strain IbAr10200, ZsGreen reporter virus expressing the  
516 fluorescence tag on the N-terminus of the genomic S-segment ORF, designated rCCHFV-  
517 ZsGreen, was used for the fluorescence reduction neutralization test (kindly provided by Dr. Éric  
518 Bergeron of Centers for Disease Control and Prevention, Atlanta, GA). CCHFV strain IbAr10200  
519 was obtained from the World Reference Collection of Emerging Viruses and Arboviruses at  
520 UTMB (WRCEVA, passaged 13 times in suckling mice and one time in Vero E6; Genbank  
521 sequences: NC005302, NC005300, and NC005301) and was passaged twice in SW-13 cells  
522 (ATCC, CCL-105) before use. All work with CCHFV was performed in a biosafety level 4 facility  
523 at the Galveston National Laboratory, University of Texas Medical Branch, Galveston, TX, in  
524 accordance with the approved Institutional Biosafety Committee protocols.

### 525 *Generation of Rhabdoviral vaccine vector cDNA*

526 The human codon-optimized CCHFV-M, IbAr10200 strain<sup>31</sup> (CCHFV-coM), used to develop the  
527 CCHFV vaccines was a generous gift from Dr. Aura Garrison (USAMRIID, Frederick, MD). All



528 BNSP333<sup>35</sup> and cVSV-XN<sup>36</sup> vectors were kindly provided by Dr. Tiago Abreu-Mota (Thomas  
529 Jefferson University, Philadelphia, PA). The chimeric GP38 protein was cloned by first PCR  
530 amplifying the human Ig $\kappa$  signal sequence with primers GSP49 and GSP53 and GP38 with  
531 primers GSP54 and GSP55. This construct was cloned into a pDisplay vector with the addition  
532 of an HA tag through In-Fusion® cloning (Takara Bio). The GP38 gene containing the Ig $\kappa$  signal  
533 sequence was then PCR amplified with primers GSP68 and GSP69, and the RABV-G tail was  
534 amplified with primers GSP70 and GSP71. Through In-fusion®, these two PCR products were  
535 combined and cloned into a pCAGGS vector. This chimeric GP38 gene was then inserted into  
536 the BNSP333 vector using restriction sites BsiWI and NheI, and the plasmid was designated  
537 BNSP333-GP38. To produce the GP85 chimeric protein, the MLD gene was PCR amplified  
538 from the original CCHFV-coM gene using primers GSP84 and GSP85, and the GP38 chimeric  
539 gene was PCR amplified using primers GSP86 and GSP71, excluding the signal sequence.  
540 This chimeric GP85 gene was cloned into a pCAGGS vector with In-fusion® cloning and finally  
541 cloned into the BNSP333 vector using restriction sites BsiWI and NheI. This resulting plasmid  
542 was designated BNSP333-GP85. All CCHFV-coM genes were PCR amplified to have 50 amino  
543 acids in the Gc cytoplasmic tail truncated as previously described<sup>42</sup>. Primers GSP03 and GSP20  
544 (GP38+ Gc+) or GSP21 (GP38- Gc+) were used to PCR amplify the CCHFV-coM for the VSV  
545 vectors, and GSP06 and GSP07 were used to PCR amplify RABV-G containing the R333E  
546 mutation (RVG-333) for the VSV vector. CCHFV-coM was inserted into the VSV vectors using  
547 either MluI and NotI (GP38- Gc+) or MluI and NheI (GP38+ Gc+) restriction sites. RVG-333 was  
548 inserted into the VSV vector containing CCHFV-coM using NotI and NheI restriction sites. The  
549 resulting plasmids were designated VSV- $\Delta$ G-CCHFV-coM-RVG (GP38- Gc+) and VSV- $\Delta$ G-  
550 CCHFV-coM (GP38+ Gc+). The sequences of these three plasmids were confirmed by  
551 sequencing using primers GSP08, GSP09, RP591, RP592, RP1325, and RP1327 for the RABV

552 vector and GSP08-GSP19, VPF5, and VP9R for the VSV vectors. Primer sequences are listed  
553 in **Table 1**.

#### 554 *Recovery of recombinant viruses*

555 Recombinant RABV and VSV vaccines were recovered as previously described<sup>58,59</sup>. Briefly, X-  
556 tremeGENE 9 (MilliporeSigma®) in Opti-MEM (Gibco®) was used to co-transfect the respective  
557 full-length viral cDNA along with the plasmids encoding RABV N, P, and L or VSV N, P, and L  
558 proteins, with the addition of RABV G for the VSV surrogate challenge virus and pCAGGs  
559 plasmids expressing T7 RNA polymerase in 293T cells in poly-l-lysine coated 6-well plates. The  
560 supernatants of RABV transfected cells were harvested every 3 days, and VSV transfected cell  
561 supernatants were harvested every 2 days. Presence of infectious RABV was detected by  
562 immunostaining for RABV N with 1:200 dilution of fluorescein isothiocyanate (FITC) anti-RABV  
563 N monoclonal globulin (Fujirebio®, product #800-092) or for virus-induced cytopathic effect  
564 (CPE) in the case of VSV.

#### 565 *Viral production and titering*

566 GP38+ Gc-, GP38- Gc+, GP38+ Gc+, Filorab1<sup>60</sup> (generous gift of Dr. Drishya Kurup, Thomas  
567 Jefferson University, Philadelphia, PA), BNSP333<sup>35</sup>, VSV-GFP (plasmid provided by Dr. Tiago  
568 Abreu-Mota), VSV-ΔG-RABV-G and SPBN<sup>35</sup> viruses were grown and titered on Vero cells.  
569 Specifically, Vero cells were cultured with VP-SFM (Gibco®) supplemented with 1% P/S, 2X  
570 GlutaMAX™ (Gibco®) and 10mM HEPES buffer (Corning®) and infected with a multiplicity of  
571 infection (MOI) of 0.01 for Filorab1, BNSP333, and VSV-GFP and 0.001 for GP38+ Gc-, GP38-  
572 Gc+, and GP38+ Gc+. GP38+ Gc+ to be used in the surrogate challenge model was grown on  
573 BSR cells in DMEM supplemented with 5% FBS and 1% P/S, infected at MOI 0.001. VSV-ΔG-  
574 RABV-G and SPBN were grown on BEAS-2B cells in OptiPRO™ SFM (Gibco™), supplemented  
575 with 1% P/S, 2X GlutaMAX™ (Gibco®) and 10mM HEPES buffer (Corning®), and infected with

576 a multiplicity of infection (MOI) of 0.01. Viruses were harvested every 3 days with VP-SFM  
577 media replacement until viral titers started to decrease for RABVs or until 80% cytopathic effect  
578 was detected for VSVs. RABV titering was performed by limiting dilution focus-forming assay  
579 using FITC anti-RABV N monoclonal globulin (Fujirebio®; catalogue number: 800-092) as  
580 previously described<sup>61</sup>. VSV titers were determined by plaque forming assay using 2% methyl  
581 cellulose overlay<sup>62</sup>.

#### 582 *Purification and virus inactivation*

583 To produce inactivated GP38+ Gc-, GP38- Gc+, GP38+ Gc+, and Filorab1 vaccines, viral  
584 supernatant was concentrated, sucrose purified<sup>63</sup>, and inactivated<sup>60</sup> as previously described.  
585 Briefly, viral supernatants with the highest titers were pooled for each virus and concentrated at  
586 least 5x in an Amicon® 300mL stirred cell concentrator using a 500 kDa exclusion PES  
587 membrane (MilliporeSigma®). Concentrated supernatants were then overlaid onto a 20%  
588 sucrose cushion and centrifuged at 76,755 x g for 2hrs. Virions pellets were resuspended in  
589 TEN buffer (100mM Tris base, 50mM NaCl, 2mM EDTA in ddH<sub>2</sub>O) with 2% sucrose and  
590 incubated overnight (O.N.) at 4°C. β-propiolactone (BPL) (MilliporeSigma®) was added at a  
591 1:2000 dilution for inactivation. Samples were left at 4°C O.N. shaking and then incubated the  
592 following day at 37°C for 30min to hydrolyze the BPL. Virus inactivation was confirmed as  
593 previously described<sup>24</sup>. Briefly, supernatant inoculated with 10µg of inactivated virions was  
594 passaged in T25 flasks of Vero cells; cells were fixed and stained with FITC anti-RABV N or  
595 monitored for cytopathic effect.

#### 596 *Immunofluorescence*

597 3E5 Vero cells were seeded on glass coverslips in a 12-well plate and infected the next day at  
598 an MOI of 0.01 with the respective viruses. After 72hrs (RABV viruses) or 24hrs (VSV viruses),  
599 cells were washed in 1X DPBS and fixed for 10mins in 2% paraformaldehyde (PFA) in 1X

600 DPBS for surface staining. Those slides to be used for intracellular staining were then fixed for  
601 an additional 15mins in 2% PFA with 0.1% Triton™ X-100 (Sigma-Aldrich®). Subsequently,  
602 cells were washed 2-3 times with 1X DPBS and blocked in 1X DPBS with 5% FBS for 1hr at  
603 room temperature or overnight at 4°C. Cells were then probed for 1hr at room temperature with  
604 primary antibodies in 1X DPBS with 1% FBS, specifically, anti-RABV-G 4C12 at 4µg/mL, with  
605 either anti-Gc 11E7 at 3.2µg/mL or anti-GP38 13G8 at 2.4µg/mL. Cells were washed once with  
606 1X DPBS and incubated with 2.5µg/mL of anti-mouse AF568 and 2.5µg/mL of anti-human  
607 AF647 in 1X DPBS with 1% FBS for 45mins at room temperature. Cells were then washed 5  
608 times with 1X DPBS, mounted onto slides using mounting media containing 4',6-diamidino-2-  
609 phenylindole (DAPI) (ProLong™ Glass Antifade Mountant, Invitrogen™ catalog number:  
610 P36980), and stored O.N. at room temperature in the dark. Slides were visualized the next day  
611 using a Nikon Ti-E microscope with Nikon A1R Laser Scanning confocal camera with the Plan  
612 Fluor 40x/1.3 objective lens on the NIS-Elements C software for multi-dimensional experiment  
613 acquisition and analysis at 23°C. Color channels were processed (channels separated for  
614 individual images and merged for merged images) using ImageJ software (OSS NIH).

#### 615 *Glycoprotein FACS analysis*

616 A total of 8E5 Vero cells for RABVs or 3e5 Vero cells for VSVs were seeded in 6-well plates.  
617 The following day, cells were infected with RABVs at MOI 10 for 48hrs or left uninfected  
618 (control). Two days later, cells were infected with VSVs at MOI 5 for 8hrs. Medium was then  
619 aspirated, and cells were washed once with 1X DPBS. Cellstripper® (Corning™, catalog  
620 number 25-056-CI) was added to each well for 5-10 min to remove the cells from the well. Cells  
621 were then transferred to 15mL conical tubes and centrifuged at 400 x g for 5 min. Cells were  
622 resuspended in 100µL per 8E5 cells of 2% PFA in 1X PBS, seeded in a 96-well round bottom  
623 plate with 8E5 cells per well, and fixed for 10 min. Cells were centrifuged at 250 x g for 3min  
624 and washed three times in 200µL FACS buffer (10% FBS and 0.05% NaN<sub>3</sub>) per well. Cells were

625 stained in 100 $\mu$ L of primary antibody mixture containing anti-RABV-G 4C12 at 4 $\mu$ g/mL and  
626 either anti-Gc 11E7 at 3.2 $\mu$ g/mL or anti-GP38 13G8 at 2.4 $\mu$ g/mL in FACS buffer O.N. at 4°C.  
627 The next day, cells were washed twice with 200 $\mu$ L FACS buffer and then stained with 100 $\mu$ L of  
628 secondary antibody mixture containing goat anti-mouse BV510 at 0.2 $\mu$ g/100 $\mu$ L and goat anti-  
629 human AF647 at 2.5 $\mu$ g/mL in FACS buffer for 2hrs at room temperature. Cells were then  
630 washed 3 times in 200 $\mu$ L FACS buffer and transferred to FACS tubes in a total of 400 $\mu$ L FACS  
631 buffer. Cells were analyzed for GFP emission to detect GFP expression (i.e., VSV-GFP  
632 infection) in the FITC channel, BV510 emission to detect CCHFV-Gc or GP38 in the BV510  
633 channel, and AF647 emission to detect RABV-G in the allophycocyanin (APC) channel using a  
634 BD FACSCelesta™ Cell Analyzer. Data analysis was performed using FlowJo software  
635 (Treestar, Ashland, OR).

#### 636 *SDS PAGE Protein Gel and Western Blot*

637 Sucrose purified virus particles and purified CCHFV glycoproteins were denatured with Urea  
638 Sample Buffer (125mM Tris-HCl [pH 6.8], 8 M urea, 4% sodium dodecyl sulfate, 0.02%  
639 bromophenol blue) and reduced with 2-mercaptoethanol (CAS No. 60-24-2, Millipore Sigma®)  
640 and boiling at 95°C for 10min. However, samples to be probed with any of the anti-CCHFV  
641 antibodies were left unreduced, as these antibodies are conformational. 1 $\mu$ g of samples for total  
642 protein analysis were resolved on a 10% SDS-PAGE gel and stained O.N. with SYPRO™ Ruby  
643 Protein Gel Stain (ThermoFisher Scientific). 1 $\mu$ g of samples for western blot analysis were  
644 resolved on a 10% SDS-PAGE gel and transferred onto a nitrocellulose membrane in Towbin  
645 buffer (192mM glycine, 25mM Tris, 20% methanol). Blots were then blocked in 5% milk  
646 dissolved in PBS-T (0.05% Tween® 20 [MilliporeSigma®]) at room temperature for 1hr. Next,  
647 membranes were incubated with primary antibody O.N. at 4°C. Antibodies were made in a  
648 solution of 5% bovine serum albumin (BSA) in PBS. Anti-Gc 11E7 was used at a dilution of  
649 320ng/mL, anti-GP38 13G8 was used at a dilution of 240ng/mL, and anti-RABV-G 4C12 was

650 used at 2µg/mL dilution. The next day the blots were washed with PBS-T and incubated with  
651 horseradish peroxidase (HRP)-conjugated anti-mouse or human IgG at 1:40,000 dilution in  
652 PBS-T for blots probed with 11E7, 1:20,000 dilution in PBS-T for blots probed with 13G8 or  
653 1:20,000 in PBS-T for blots probed with 4C12. Proteins were detected with SuperSignal West  
654 Dura Chemiluminescent substrate (Pierce®) and imaged on the FluorChem R system  
655 (proteinsimple®).

#### 656 *Multi-step and One-step Growth Curves*

657 Vero E6 cells were seeded in 6-well plates at 7E5 cells/well. The following day, cells were  
658 checked for 70% confluency and then infected in serum free medium at MOI 0.01 for multi-step  
659 growth curves or MOI 10 for one-step growth curves. After two hours of incubation, the media  
660 was aspirated, and the infected cells were washed 2X with 1X DPBS (Corning®). DMEM  
661 supplemented with 5% FBS and 1% P/S was added to each well, and the first sample of 200µL  
662 was taken from each well. Samples were taken every 24hrs until 120hrs post-infection for  
663 RABVs and at 2, 4, 6, 8, 12, 24, 36, and 48hrs post-infection for VSVs. Each viral sample was  
664 titered in triplicate as described above in the *Viral production and titering* section.

#### 665 *Immunizations*

666 Groups of five 6- to 10-week-old male and female C57BL/6 mice were immunized  
667 intramuscularly (I.M.) with 10µg BPL-inactivated virus (see **Figure 3a** for dose schedule)  
668 formulated alone in PBS or with the addition of Synthetic Monophosphoryl Lipid A (MPLA),  
669 3D(6A)-PHAD, in a squalene-in-oil emulsion (PHAD-SE), at a dose of 5µg PHAD and 2% SE.  
670 Each immunization was administered as a total of 100µL, with 50µL injected in each hind leg  
671 muscle. Serum was collected through retro-orbital bleeds performed under isoflurane  
672 anesthesia on days 0, 14, 28, 35, and 42, with the final bleed on day 56.

#### 673 *Production of ELISA antigens*

674 RABV-G antigen was produced as previously described<sup>50</sup>. Briefly, BEAS-2B cells were infected  
675 with VSV-ΔG-GFP-RABV-G (for RABV vaccines) or SPBN (for VSV vaccines) in Opti-PRO  
676 (Gibco®). Viral supernatants were concentrated and purified as described above in the  
677 purification section. After sucrose purification, viral pellets were resuspended in TEN buffer  
678 (100mM NaCl, 100mM Tris, 10mM EDTA pH7.6) containing 2% OGP (Octyl-β-D-  
679 glucopyranoside) detergent and incubated for 30min at room temperature while shaking. This  
680 mixture was centrifuged at 3000 x g for 10min, supernatant collected and further centrifuged at  
681 25,000 x g for 90min. Supernatant was collected and analyzed for presence of antigen via  
682 western blot with anti-RABV-G antibody.

683 CCHFV- Gc HA-tagged antigen was prepared as previously described for other HA-tagged  
684 antigens<sup>24</sup>. Subconfluent T175 flasks of 293 T cells that were poly-l-lysine coated were  
685 transfected with a eukaryotic expression vector (pDisplay) encoding for each individual CCHFV  
686 glycoprotein with the cleavage sites and transmembrane regions removed, specifically amino  
687 acids 1040 to 1631 of CCHFV-M, fused to a C-terminal hemagglutinin (HA) peptide.  
688 Supernatant was collected one week after transfection, clarified by centrifugation, and filtered  
689 through a 0.45um filter before being loaded onto an equilibrated anti-HA agarose column  
690 (Pierce) containing either a 2.5mL or 5mL agarose bed volume. The supernatant was allowed to  
691 bind to the column overnight at 4°C. The following day, the column was washed with 10-bed  
692 volumes of PBS-T, and bound HA-tagged glycoprotein was eluted with 5-10mL of 0.4mg/mL HA  
693 peptide in PBS. Fractions were collected and analyzed for the presence of Gc glycoprotein  
694 through western blot with CCHFV-Gc 11E7 antibody. Peak fractions were pooled and dialyzed  
695 against PBS in 10,000 molecular weight cutoff dialysis cassettes (MWCO) (Thermo Scientific™)  
696 to remove excess HA peptide. After dialysis, the protein was quantified by nanodrop 2000c  
697 spectrophotometer and/or bicinchoninic acid (BCA) assay. Halt™ Protease Inhibitor Cocktail  
698 (Thermo Scientific™, catalog number: 78430) was added for a final concentration of 1X and

699 sodium azide ( $\text{NaN}_3$ ) added for a final concentration of 0.05% before freezing the protein in  
700 small aliquots at  $-80^\circ\text{C}$ .

701 CCHFV-GP38 Strep-tagged antigen was prepared from an enhanced expression vector (pEEV)  
702 containing the sequence for CCHFV-GP85 strain IbAr10200 from amino acids 22 to 515, with a  
703 N-terminal FLAG and His tag and a C-terminal Strep-Tag II (referred to as pEEV-HisFlag-GP85-  
704 10200-Strep) (generously provided by Dr. Éric Bergeron at the Centers for Disease Control,  
705 Atlanta, GA). The plasmid pLEX307-FURIN-puro (ID # 158460), containing the human furin  
706 gene was ordered from AddGene. This gene was then PCR amplified with primers GSP87 and  
707 GSP88 and cloned into a pCAGGS vector through In-Fusion™ cloning. 293F cells were grown  
708 in FreeStyle™ 293 Expression Medium (Gibco®) with 2X Glutamax (Gibco®) and seeded at  
709  $3 \times 10^6$  cells/mL in Erlenmeyer flasks. The next day, cells were transfected using FectoPRO®  
710 (Polyplus transfection™) transfection reagent following the reagent manual with slightly altered  
711 conditions. The pEEV-HisFlag-GP85-10200-Strep and pLEX307-FURIN-puro plasmids were  
712 transfected at a ratio of 4:1 in a total of  $0.8\mu\text{g}$  plasmid DNA for each ml of culture. This co-  
713 transfection with the furin plasmid was to ensure that the MLD was cleaved from GP38. Media  
714 for the transfection complexes was 1/10 of the total culture volume and  $1.5\mu\text{L}$  of FectoPro  
715 reagent was used per  $\mu\text{g}$  of DNA. 4 hours after transfection, FectoPRO® booster was added in  
716 an equivalent amount to that of DNA (i.e.,  $0.8\mu\text{g/mL DNA} = 0.8\mu\text{L FectoPRO® booster/mL}$ ).  
717 Cells were incubated until cell viability sharply declined, typically around 3 days post  
718 transfection. The supernatant was then harvested, spun down for 30mins at  $4000 \times g$  and  
719 filtered through a  $0.45\mu\text{m}$  filter before being loaded onto a column with a 2mL bed volume of  
720 Strep-Tactin®XT resin (IBA Lifesciences). The supernatant was allowed to bind to the column  
721 overnight at  $4^\circ\text{C}$ . The following day, the column was washed with 5 column bed volumes of 1X  
722 Buffer W (IBA Lifesciences) and then eluted with 6X 0.5 column bed volumes of 1X Buffer BXT  
723 (IBA Lifesciences), collected as 0.5mL fractions. Fractions were analyzed for the presence



724 CCHFV-GP38 through western blot with CCHFV-Gc 13G8 antibody. The protein was quantified  
725 by nanodrop 2000c spectrophotometer and/or bicinchoninic acid (BCA) assay. Halt™ Protease  
726 Inhibitor Cocktail (Thermo Scientific™, catalog number: 78430) was added for a final  
727 concentration of 1X and sodium azide (NaN<sub>3</sub>) added for a final concentration of 0.05% before  
728 freezing the protein in small aliquots at -80°C.

729 *Enzyme-linked immunosorbent assay (ELISA)*

730 Individual mouse serum was analyzed by ELISA for the presence of IgG specific to CCHFV-  
731 GP38, -Gc, and RABV-G. Antigens were diluted in coating buffer (15mM Na<sub>2</sub>CO<sub>3</sub>, 35mM  
732 NaHCO<sub>3</sub> [pH 9.6]) at a concentration of 100ng/well (1ng/μL) for GP38, 150ng/well (1.5ng/μL) for  
733 Gc, and 50ng/well (0.5ng/μL) for RABV-G, and then 100μL was added to each well of 96-well  
734 immulon 4HBX plates (Nunc®) and incubated O.N. at 4°C. The following day, plates were  
735 washed three times with PBS-T (0.05% Tween 20 in 1X PBS), blocked for 2hrs (5% milk in  
736 PBS-T), and washed again three times with PBS-T. Sera or control mAbs were diluted in three-  
737 fold serial dilutions (starting with a 1:50 dilution or higher dilutions of 1:150, 1:450, or 1:1350 for  
738 sera that did not reach endpoint titer) down the plate in 1X PBS with 0.5% BSA and incubated  
739 O.N. at 4°C. Plates were then washed three times with PBS-T and 100μL secondary antibody  
740 HRP conjugated goat anti-mouse IgG Fc at a concentration of 50ng/mL for GP38 and Gc, and  
741 25ng/mL for RABV-G in PBS-T was added to each well and incubated for 2hrs at room  
742 temperature. For isotype subclass ELISAs, the appropriate secondary antibody was used at the  
743 same concentration as the IgG Fc-specific secondary antibody. Then plates were washed three  
744 times with PBS-T, and 200μL of o-phenylenediamine dihydrochloride (OPD) substrate  
745 (ThermoFisher®) was added and left incubating for 15 min for GP38 and Gc and 13 min for  
746 RABV-G. The reaction was stopped by adding 50μL of 3M Sulfuric acid (H<sub>2</sub>SO<sub>4</sub>). Optical density  
747 was determined at 490nm (OD490) and 630nm (OD630) and delta values calculated subtracting  
748 the background OD630 readings from the OD490 readings. ELISA data was analyzed with

749 GraphPad Prism 8 using a sigmoidal nonlinear fit (4PL regression curve) model to determine  
750 the half maximal Effective Concentration ( $EC_{50}$ ) serum or antibody titer. An accurate  $EC_{50}$  value  
751 cannot be calculated without a full curve, therefore samples without a proper curve are  
752 considered to have no detectable antibodies against that antigen and have a reported  $EC_{50}$  of 1.  
753 Isotype ratios were calculated by taking either the IgG2c or IgG2b  $EC_{50}$  value, dividing it by the  
754 IgG1  $EC_{50}$  value. For those samples where there was no detectable IgG1 antibodies, no isotype  
755 ratio could be calculated. Positive controls (when available) for each assay were as follows:  $\alpha$ -  
756 CCHFV-GP38 13G8 for IgG Fc and IgG2b GP38 ELISAs;  $\alpha$ -CCHFV-GP38 10E11 for IgG1  
757 GP38 ELISAs;  $\alpha$ -CCHFV-Gc 11E7 for IgG Fc Gc ELISAs;  $\alpha$ -RABV-G 1C5 for IgG Fc RABV-G  
758 ELISAs.

#### 759 *Surrogate CCHFV challenge virus Pathogenicity*

760 Groups of five 8–10-week-old male interferon  $\alpha/\beta$  receptor 1 knockout (IFNAR<sup>-/-</sup>) mice were  
761 infected with various doses of GP38+ Gc+ I.P. (200 $\mu$ L total) to determine the parameters  
762 needed for use as a challenge model. The virus was diluted in PBS for all doses. Mice were  
763 weighed daily and monitored for signs of disease until day 14 post-infection. Mice that lost more  
764 than 20% of their starting weight or appeared moribund were humanely euthanized. Blood was  
765 collected at days 0, 4, and 14 to be used for in a VSV-N qPCR to look for viremia.

#### 766 *Surrogate CCHFV challenge model in mice*

767 Groups of five 8- to 10-week-old male and female IFNAR<sup>-/-</sup> mice were immunized i.m. with 10 $\mu$ g  
768 of BPL inactivated GP38+ Gc- or FR1 vaccines adjuvanted with 5 $\mu$ g PHAD in 2% SE at days 0  
769 and 28 (**Figure 7a**). On day 65, mice were injected with 5e5pfu of GP38+ Gc+ diluted in PBS as  
770 determined above. Mice were sacrificed: (1) when weight loss reached  $\geq 20\%$  or (2) if severe  
771 clinical signs of disease were observed. Terminal bleeding was collected upon sacrifice when  
772 possible. Mice were bled at days 0, 4, and 14 to look for viremia in a VSV-N qPCR.

773 *RNA Extraction*

774 50µL of whole blood was added to 300µL of TRIzol LS Reagent (Life Technologies) and 50µL of  
775 DPEC water, or 250µL of virus supernatant was added to 750µL of TRIzol LS Reagent. The  
776 protocol for RNA extraction of biological fluids with TRIzol LS Reagent was used up to the  
777 phase separation step. Then the protocol from the PureLink RNA Mini Kit (Ambion) was used  
778 for the remainder of the extraction. A NanoDrop (Fisher) was used to measure the concentration  
779 and quality (260/280 ratios) of extracted RNA.

780 *Measuring Surrogate Challenge Virus Viremia via quantitative Real-Time polymerase chain*  
781 *reaction (qPCR)*

782 First, VSV-N RNA was prepared to act as a standard for the qPCR. RNA was isolated from  
783 GP38+ Gc+ virus and cDNA produced using the One-Step RT PCR (SuperScript IV, Thermo  
784 Fisher Scientific) with primers GSP66 and GSP67. This cDNA was used to produce RNA  
785 standards via *in-vitro* transcription using the MEGAscript® T7 Kit (Invitrogen™) followed by the  
786 MEGAclean™ Transcription Clean-Up Kit (Invitrogen™). The qPCR was then run following the  
787 protocol for TaqMan Fast Virus 1 Step Master Mix reagent (ThermoFisher), using 5µL of RNA  
788 per reaction, primers GSP72 and GSP74, and probe GSP73 with a 60°C annealing  
789 temperature. Any day 0 samples showing detectable viral RNA were considered contaminated  
790 and not reported. Full primer and probe sequences are listed in **Table 1**.

791 *Wildtype CCHFV challenge in IFNAR<sup>-/-</sup> mice*

792 Mice were challenged with 1000pfu of CCHFV strain IbAr10200 by intraperitoneal (i.p.) route as  
793 previously described<sup>64</sup>. Virus was diluted in a total volume of 0.1 ml of PBS (Gibco). All mice  
794 were injected i.p. with a total of 2.5 mg of anti-IFNAR 1 (mAb-5A3; Leinco Technologies Inc.)  
795 diluted in PBS 24 hours before (2.0 mg) and 24 hours after infection (.5 mg) in a total volume of

796 0.2 ml. Mice were observed at least daily and weighed for the first 10 days daily and then every  
797 3 days.

798 *Wildtype CCHFV FRNT*

799 Mouse sera were serially diluted 1:2 in serum-free DMEM then incubated with rCCHFV-  
800 ZsGreen virus for 1 hour on ice. The mixture was inoculated onto wells of HuH-7 cells and  
801 incubated for 1 hour at 37°C with 5% CO<sub>2</sub>. Cells were then supplemented with D10 and  
802 incubated until 48 hours post infection. Relative fluorescence of each well was measured on a  
803 GFP plate reader. Wells inoculated with rCCHFV-ZsGreen virus only served as the control for  
804 maximum fluorescence, and wells inoculated with serum-free DMEM without virus served as the  
805 control for background fluorescence. Percent virus neutralization was calculated from the  
806 percent of fluorescence reduction from serum plus virus wells compared to virus only wells.  
807 IC<sub>50</sub> values were determined using a four parameter, variable slope, nonlinear regression  
808 model in GraphPad PRISM.

809 *Rapid Fluorescent Focus Inhibition Test (RFFIT)*

810 RFFIT neutralization assay was performed as previously described<sup>65</sup>. Briefly, serum was heat  
811 inactivated at 56°C for 30 mins. NA cells were seeded at 3E4 cells per well in a 96-well plate. 2  
812 days later, serum samples were diluted in a 2-fold dilution series in Opti-MEM in 96-well plates  
813 at a starting dilution of 1:40 (unless stated otherwise). The US standard rabies immune globulin  
814 (WHO Standard) was used at a starting dilution of 2IU/mL. A dilution of CVS-11 previously  
815 determined to produce 90% infection was added to each well with either sera or the WHO  
816 Standard and incubated for 1hr at 34°C. The media in the plates with the NA cells was then  
817 replaced by the sera/virus mixture and incubated for 2hrs at 34°C. This media was aspirated,  
818 and fresh Opti-MEM was added. Plates were incubated for 22hrs at 34°C and then fixed with  
819 80% acetone and stained with FITC-conjugated anti-RABV-N antibody for at least 4 hours. The

820 Reed-Muench method was used to calculate 50% endpoint titers, which were subsequently  
821 converted to international units (IU) per milliliter through comparison to the WHO standard.

### 822 *Statistical analysis*

823 All statistical analysis was performed using GraphPad Prism 8 on log transformed data. For  
824 growth curves, each time point was compared to the parental vector control using the ordinary  
825 one-way ANOVA with the Tukey Multiple Comparison Test. The Mann Whitney test was used  
826 for comparison within two groups at each timepoint for all ELISA EC<sub>50</sub> data and IU/mL RFFIT  
827 data. For groups analysis at each time point of ELISA EC<sub>50</sub> titers, IU/mL RFFIT data, and qPCR  
828 viral RNA copies, an ordinary one-way ANOVA was used with a post-Hoc analysis using Tukey  
829 Multiple Comparison Test with a 95% confidence interval. To look at the differences in group  
830 average weight change over time for the surrogate challenge virus, a two-way ANOVA was  
831 used with Tukey's Multiple Comparisons Test. A two-way ANOVA was used with a Dunnett  
832 multiple comparisons test to compare differences in weight loss over time to the control female  
833 PBS group for the WT CCHFV challenge. The log-rank Mantel-Cox test was performed to  
834 compare differences in survival to the control female PBS group.

**Table 1. Primer Sequences**

Primer	Direction	Sequence	Use
GSP03	Forward	5'- CGATCTGTTTACGCGTGCCACCATGCACATC AGCC-3'	PCR amplification of CCHFV-coM for insertion into VSV vectors. Primer contains MluI restriction site.
GSP06	Forward	5'- AGATATCACGCTCGAGGCCACCATGGTTCC TCAGG-3'	PCR amplification of RVG-333 for insertion into VSV vector. Primer contains NotI restriction site.
GSP07	Reverse	5'- GAAGAATCTGGCTAGCTTACAGTCTGGTCT CACCCC-3'	PCR amplification of RVG-333 for insertion into VSV vector. Primer contains NheI restriction site.
GSP08	Reverse	5'-CTCGCCGGTGATGAAGAACT-3'	CCHFV-coM sequencing primer.
GSP09	Forward	5'- ACCCTGTGAGAAACCTGCTG-3'	CCHFV-coM sequencing primer.
GSP10	Reverse	5'- TTGATCACGCAGTCGGTGAA-3'	CCHFV-coM sequencing primer.
GSP11	Forward	5'- CCTGAAGGCCAGCATCTTCA-3'	CCHFV-coM sequencing primer.
GSP12	Reverse	5'- GCAGTAGGGGCAGATGTTGT-3'	CCHFV-coM sequencing primer.
GSP13	Forward	5'- GGCGATATCCTGGTGGACTG-3'	CCHFV-coM sequencing primer.
GSP14	Reverse	5'- CAGTGTCTGCAGTAAGGGC-3'	CCHFV-coM sequencing primer.
GSP15	Forward	5'-TGCCCTTACTGCAGACTG-3'	CCHFV-coM sequencing primer.
GSP16	Reverse	5'- ATGTTTCTGGGCTCGGACAG-3'	CCHFV-coM sequencing primer.
GSP17	Forward	5'- TCAACGTGCAGTCCACCTAC-3'	CCHFV-coM sequencing primer.
GSP18	Reverse	5'- TCCTCCTCGCTACAGCTCTT-3'	CCHFV-coM sequencing primer.
GSP19	Forward	5'- AAGAGCTGTAGCGAGGAGGA-3'	CCHFV-coM sequencing primer.
GSP20	Reverse	5'-GCTAGCTTAGCCTCTGGTTCTCCG-3'	PCR amplification of CCHFV-coM for insertion into VSV-ΔG vector for surrogate challenge virus. Primer contains NheI restriction site.
GSP21	Reverse	5'-GCGGCCGCTTAGCCTCTGGTTCTCCG-3'	PCR amplification of CCHFV-coM for insertion into VcoM vector for vaccine. Primer contains NotI restriction site.
GSP42	Reverse	5'-CATAGTCATCTTCATTGA-3'	Sequencing primer for RVG in VSV-ΔG-coM-RVG.
GSP49	Forward	5'- GCCGCCAGTGTGCTGGAATTCGCCACCATG GAGACAGACACA-3'	PCR amplification of signal sequence for GP38 chimeric gene.
GSP53	Reverse	5'- tcttcaggttGTCACCAGTGGAACTGGAACC- 3'	PCR amplification of signal sequence for GP38.
GSP54	Forward	5'-CACTGGTGACaacctgaagatggagatca-3'	PCR amplification of GP38 for GP38 with a signal sequence.
GSP55	Reverse	5'-	PCR amplification of GP38 for GP38 with a signal sequence.

		AACATCGTATGGATAGTCGACGGACCCGGT GCTGGCCTT-3'	
GSP66	Forward	5'- TAATACGACTCACTATAGGGGGACAGCCTG ATGACATTG-3'	Primer for IVT of VSV-N.
GSP67	Reverse	5'-TCTGGTGCATACAAACCT-3'	Primer for IVT of VSV-N.
GSP68	Forward	5'- CAAAGAATTCCGGAACGTACGGCCACCATG GAGACAGACACA -3'	PCR amplification to put the GP38 with the signal sequence into a pCAGGS plasmid.
GSP69	Reverse	5'-CCGAGGATTCGGACCCGGTGCTGGCCTT -3'	PCR amplification to put the GP38 with the signal sequence into a pCAGGS plasmid.
GSP70	Forward	5'- CACCGGGTCCGAATCCTCGGTTATCCCC -3'	PCR amplification of RABV-G 51 amino acids of the ectodomain (ED51), transmembrane domain (TM) and cytoplasmic tail (CT) to make the chimeric GP38.
GSP71	Reverse	5'- GAGGGAAAAAGATCTGCTAGCTTACAGTCT GGTCTCACCCCC -3'	PCR amplification of RABV-G 51 amino acids of the ectodomain (ED51), transmembrane domain (TM) and cytoplasmic tail (CT) to make the chimeric GP38.
GSP72	Forward	5'-CCTCTGCCGACTTGGCACAA-3'	Primer for qPCR of VSV-N.
GSP73	Probe	5'- CCGAGGATTGACGACTAATGCACCGCCAC AAGGCAG-3'	Primer-probe for qPCR of VSV-N.
GSP74	Reverse	5'-CCGAGCCATTCGACCACATC-3'	Primer for qPCR of VSV-N.
GSP84	Forward	5'- CAAAGAATTCCGGAACGTACGATGCACATC AGCCTGATGTACGC -3'	PCR amplification of MLD to create the chimeric GP85.
GSP85	Reverse	5'- TCTTCAGGTTCCGCTTGCTCCTGTTGGTGG -3'	PCR amplification of MLD to create the chimeric GP85.
GSP86	Forward	5'- GAGCAAGCGGAACCTGAAGATGGAGATCA TCCTGA -3'	PCR amplification of chimeric GP38 to create the chimeric GP85.
GSP87	Forward	5'- AATTCGGAACGTACGGCCACCATGGAGCT GAGG-3'	PCR amplification of human furin gene to insert into pCAGGS plasmid.

GSP88	Reverse	5'- AAAAAGATCTGCTAGCTTAGAGGGCGCTCT GGTC-3'	PCR amplification of human furin gene to insert into pCAGGS plasmid.
RP591	Forward	5'-GGAGGTCGACTAAAGAGATCTC ACATAC-3'	Sequencing of foreign gene in BNSP333 vector.
RP592	Reverse	5'-TTCTTCAGCCATCTCAAGATCGG CCAGAC-3'	Sequencing of foreign gene in BNSP333 vector.
RP1325	Forward	5'-GTTATGGTGCCATTAAACCGC TG-3'	Sequencing of RVG in BNSP333 vector.
RP1327	Reverse	5'-TCTCCAGGATCGAGCATCTT-3'	Sequencing of RVG in BNSP333 vector.
VP5F	Forward	5'-GCGTGGGTCCTGGATTCTAT-3'	Sequencing of foreign gene in VSV vector
VP9R	Reverse	5'-ATCGAGGGAATCGGAAGAGA AT-3'	Sequencing of foreign gene in VSV vector

836

837



838 **Supplemental Figure Legends**

839

840 **Supplemental Figure 1. Raw data for figure 2C and 2D.** Histograms and numerical values of  
841 flow cytometry staining of infected cells. Vero E6 cells were infected with RABVs at MOI 10 for  
842 48hrs or VSVs at MOI 5 for 8hrs and then fixed. Cells were then probed with  $\alpha$ -RABV-G 4C12  
843 and  $\alpha$ -CCHFV-Gc 11E7 (A) or  $\alpha$ -CCHFV-GP38 13G8 (B) and analyzed by flow cytometry.  
844 Experiment was performed multiple times, and this is one representative experiment.

845 **Supplemental Figure 2. Raw files for figure 2E and 2F.** (A, B) SDS PAGE protein gel of  
846 sucrose purified virions. 1 $\mu$ g of sucrose purified virions were run on the gel and stained with  
847 SYPRO™ Ruby stain. (A) Gel that was used for RABVs in figure 2E. (B) Gel that was used for  
848 VSVs in figure 2E. (C) Western blot of sucrose purified virions. 1 $\mu$ g of sucrose purified virions  
849 were run on an SDS PAGE gel and transferred to a nitrocellulose membrane for western  
850 blotting. Blots were either probed with  $\alpha$ -CCHFV-GP38 13G8 (top panel),  $\alpha$ -CCHFV-Gc 11E7  
851 (middle panel) or  $\alpha$ -RABV-G 4C12 (bottom panel). Image on the left is the merge of both visible  
852 and chemiluminescent channels to be able to see the ladder. Image on the right is just the  
853 chemiluminescent channel.

854 **Supplemental Figure 3. The Mucin-Like Domain is important for GP38 Processing.** (A)  
855 Schematic of BNSP333-GP38 vaccine construct with chimeric GP38/RABV-G pop out to show  
856 the individual domains of the RABV-G tail. (B) Immunofluorescence staining of infected cells.  
857 Vero E6 cells were infected with either BNSP333-GP38 or BNSP333-GP85 at MOI 0.01 for  
858 72hrs and then fixed. Cells used for Intracellular staining were permeabilized with 0.1% Triton™  
859 X-100 following fixation. Cells were then stained with  $\alpha$ -RABV-G 4C12 (purple) and  $\alpha$ -CCHFV-  
860 GP38 13G8 (red) and mounted with mounting media containing a nuclear DAPI stain (blue). In  
861 the merged images, areas where there is overlapping expression of RABV-G and CCHFV-GP38  
862 are pink. (C) Histograms and numerical values of flow cytometry staining of infected cells. Vero

863 E6 cells were infected with either BNSP333-GP38 or BNSP333-GP85 at MOI 10 for 48hrs and  
864 then fixed. Cells were then probed with  $\alpha$ -RABV-G 4C12 and  $\alpha$ -CCHFV-GP38 13G8 and  
865 analyzed by flow cytometry. Experiment was performed multiple times, and this is one  
866 representative experiment. (D) Western blot of sucrose purified virions. 1 $\mu$ g of sucrose purified  
867 virions were run on an SDS PAGE gel and transferred to a nitrocellulose membrane for western  
868 blotting. Blots were probed with  $\alpha$ -CCHFV-GP38 13G8. The image on the left is the merge of  
869 the visible and chemiluminescent channels to show the visible ladder markers, while the image  
870 on the right is just the chemiluminescent channel alone.

871 **Supplemental Figure 4. The adjuvant PHAD-SE boosts the antibody response of the**  
872 **vaccines.**  $\alpha$ -CCHFV-GP38 total IgG ELISAs for sera from GP38+ Gc- (A) and GP38+ Gc+ (B)  
873 immunized mice. EC<sub>50</sub> titers are compared over time between mice receiving unadjuvanted  
874 (solid symbols) and adjuvanted (clear symbols) vaccines. Error bars indicate the mean with  
875 standard deviation (SD) for groups of 5 mice with samples run in duplicate. The Mann-Whitney  
876 nonparametric t Test was used to determine statistical differences between groups at each time  
877 point. (\*\*\*\* $P < 0.0001$ ; \*\*\* $P < 0.0002$ ; \*\* $P < 0.0021$ ; \* $P < 0.0332$ ; ns = not significant).

878 **Supplemental Figure 5. Individual group weight curves of mice challenged with the**  
879 **surrogate challenge virus.** Curves represent the percent change in weight from the day of  
880 challenge. Dotted line represents 20% weight loss, the point at which mice were euthanized.  
881 Results show the combination of two independent experiments; hollow symbols with a dotted  
882 connecting line represent the first experiment, and symbols with a black outline and solid  
883 connecting line represent the second experiment. Females from experiment two in panel A had  
884 their cage flooded on day 3, and thus the weights at this timepoint were excluded.

885

886 **Supplemental Figure 6. Rhabdoviral-based CCHFV vaccines show no difference in**  
887 **immune responses between B6 males and females.** Total IgG ELISAs against GP38 (A) or  
888 Gc (B) with sera from mice immunized for the CCHFV WT challenge experiment. Error bars  
889 indicate the mean with standard deviation (SD) for groups of 5 mice with samples run in  
890 duplicate. An ordinary one-way ANOVA with Tukey's Multiple Comparison Test was used to  
891 determine statistical differences between groups at each time point. All groups with detectable  
892 antibody titers have 4-star significance compared to groups where no antibody titers were  
893 detected ( $****P < 0.0001$ ;  $***P < 0.0002$ ;  $**P < 0.0021$ ;  $*P < 0.0332$ ; ns = not significant).

894 **Supplemental Figure 7. Clinical score heat maps from WT CCHFV challenge.** Mice were  
895 given a clinical score from 1-4 that is represented by colors in the bars next to the heat maps.  
896 Each row represents an individual mouse, labeled based on their group and ear notches.  
897 Criteria for scores are listed in the table below the heat maps. Any time point where mice were  
898 not observed are crossed out with a gray X.

899 **References**

- 900 1 Hoogstraal, H. THE EPIDEMIOLOGY OF TICK-BORNE CRIMEAN-CONGO HEMORRHAGIC FEVER IN  
 901 ASIA, EUROPE, AND AFRICA. *Journal of Medical Entomology* **15**, 307-417 (1979).
- 902 2 World Health, O. Crimean Congo haemorrhagic fever virus fact sheet. **208** (2013).
- 903 3 Ergönül, Ö. Crimean-Congo haemorrhagic fever. *The Lancet Infectious Diseases* **6**, 203-214,  
 904 doi:10.1016/S1473-3099(06)70435-2 (2006).
- 905 4 Vorou, R., Pierrotsakos, I. N. & Maltezou, H. C. Crimean-Congo hemorrhagic fever. *Current*  
 906 *Opinion in Infectious Diseases* **20** (2007).
- 907 5 Bente, D. A. *et al.* Crimean-Congo hemorrhagic fever: History, epidemiology, pathogenesis,  
 908 clinical syndrome and genetic diversity. *Antiviral Research* **100**, 159-189,  
 909 doi:10.1016/j.antiviral.2013.07.006 (2013).
- 910 6 Gray, J. S., Dautel, H., Estrada-Pena, A., Kahl, O. & Lindgren, E. Effects of climate change on ticks  
 911 and tick-borne diseases in Europe. *Interdiscip Perspect Infect Dis* **200** (2009).
- 912 7 Estrada-Pena, A., Ayllon, N. & De La Fuente, J. Vol. 3 64-64 (2012).
- 913 8 Dowall, S. D., Carroll, M. W. & Hewson, R. Development of vaccines against Crimean-Congo  
 914 haemorrhagic fever virus. *Vaccine* **35**, 6015-6023, doi:10.1016/j.vaccine.2017.05.031 (2017).
- 915 9 Rodriguez, S. E. *et al.* Vesicular Stomatitis Virus-Based Vaccine Protects Mice against Crimean-  
 916 Congo Hemorrhagic Fever. *Scientific Reports* **9**, 7755-7755, doi:10.1038/s41598-019-44210-6  
 917 (2019).
- 918 10 Appelberg, S. *et al.* Nucleoside-modified mRNA vaccines protect IFNAR  $-/-$  mice against Crimean  
 919 Congo hemorrhagic fever virus infection. *Journal of Virology*, doi:10.1128/JVI.01568-21 (2021).
- 920 11 Mousavi-Jazi, M., Karlberg, H., Papa, A., Christova, I. & Mirazimi, A. Healthy individuals' immune  
 921 response to the Bulgarian Crimean-Congo hemorrhagic fever virus vaccine. *Vaccine* **30**, 6225-  
 922 6229, doi:10.1016/j.vaccine.2012.08.003 (2012).
- 923 12 Canakoglu, N. *et al.* Immunization of Knock-Out  $\alpha/\beta$  Interferon Receptor Mice against High  
 924 Lethal Dose of Crimean-Congo Hemorrhagic Fever Virus with a Cell Culture Based Vaccine. *PLOS*  
 925 *Neglected Tropical Diseases* **9**, e0003579-e0003579 (2015).
- 926 13 Hinkula, J. *et al.* Immunization with DNA Plasmids Coding for Crimean-Congo Hemorrhagic Fever  
 927 Virus Capsid and Envelope Proteins and / or Virus-Like Particles. *Journal of Virology* **91**, 1-19,  
 928 doi:10.1140/epjds7 (2017).
- 929 14 Aligholipour Farzani, T. *et al.* Co-Delivery Effect of CD24 on the Immunogenicity and Lethal  
 930 Challenge Protection of a DNA Vector Expressing Nucleocapsid Protein of Crimean Congo  
 931 Hemorrhagic Fever Virus. *Viruses* **11**, doi:10.3390/v11010075 (2019).
- 932 15 Suschak, J. J. *et al.* A CCHFV DNA vaccine protects against heterologous challenge and  
 933 establishes GP38 as immunorelevant in mice. *NPJ vaccines* **6**, 31-31, doi:10.1038/s41541-021-  
 934 00293-9 (2021).
- 935 16 Hawman, D. W. *et al.* A DNA-based vaccine protects against Crimean-Congo haemorrhagic fever  
 936 virus disease in a Cynomolgus macaque model. *Nature Microbiology*, doi:10.1038/s41564-020-  
 937 00815-6 (2020).
- 938 17 Buttigieg, K. R. *et al.* A novel vaccine against Crimean-Congo Haemorrhagic Fever protects 100%  
 939 of animals against lethal challenge in a mouse model. *PLoS one* **9**, e91516-e91516,  
 940 doi:10.1371/journal.pone.0091516 (2014).
- 941 18 Scher, G. & Schnell, M. J. Rhabdoviruses as vectors for vaccines and therapeutics. *Current*  
 942 *opinion in virology* **44**, 169-182, doi:10.1016/j.coviro.2020.09.003 (2020).

- 943 19 Mebatsion, T., Schnell, M. J., Cox, J. H., Finke, S. & Conzelmann, K. K. Highly stable expression of  
944 a foreign gene from rabies virus vectors. *Proceedings of the National Academy of Sciences of the*  
945 *United States of America* **93**, 7310-7314, doi:10.1073/pnas.93.14.7310 (1996).
- 946 20 Schnell, M. J., Buonocore, L., Kretzschmar, E., Johnson, E. & Rose, J. K. Foreign glycoproteins  
947 expressed from recombinant vesicular stomatitis viruses are incorporated efficiently into virus  
948 particles. *Proceedings of the National Academy of Sciences of the United States of America* **93**,  
949 11359-11365, doi:10.1073/pnas.93.21.11359 (1996).
- 950 21 Willet, M. *et al.* Preclinical Development of Inactivated Rabies Virus–Based Polyvalent Vaccine  
951 Against Rabies and Filoviruses. *The Journal of Infectious Diseases* **212**, S414-S424,  
952 doi:10.1093/infdis/jiv251 (2015).
- 953 22 Abreu-Mota, T. *et al.* Non-neutralizing antibodies elicited by recombinant Lassa–Rabies vaccine  
954 are critical for protection against Lassa fever. *Nature Communications* **9**, 4223-4223,  
955 doi:10.1038/s41467-018-06741-w (2018).
- 956 23 Keshwara, R. *et al.* A Recombinant Rabies Virus Expressing the Marburg Virus Glycoprotein Is  
957 Dependent upon Antibody-Mediated Cellular Cytotoxicity for Protection against Marburg Virus  
958 Disease in a Murine Model. *Journal of virology* **93**, e01865-01818, doi:10.1128/JVI.01865-18  
959 (2019).
- 960 24 Kurup, D., Wirblich, C., Feldmann, H., Marzi, A. & Schnell, M. J. Rhabdovirus-Based Vaccine  
961 Platforms against Henipaviruses. *Journal of Virology* **89**, 144-154, doi:10.1128/jvi.02308-14  
962 (2015).
- 963 25 Geisbert, T. W. *et al.* Vesicular stomatitis virus-based vaccines protect nonhuman primates  
964 against aerosol challenge with Ebola and Marburg viruses. *Vaccine* **26**, 6894-6900,  
965 doi:10.1016/j.vaccine.2008.09.082 (2008).
- 966 26 Mansfield, K. L. *et al.* Rabies pre-exposure prophylaxis elicits long-lasting immunity in humans.  
967 *Vaccine* **34**, 5959-5967, doi:<https://doi.org/10.1016/j.vaccine.2016.09.058> (2016).
- 968 27 Clinical Trials Registry India. *Intramuscular inactivated rabies vector platform Corona Virus*  
969 *Vaccine (rDNA-BBV151)*,  
970 <<http://ctri.nic.in/Clinicaltrials/showallp.php?mid1=58694&EncHid=&userName=035425>>  
971 (2021).
- 972 28 Whitehouse, C. A. Crimean–Congo hemorrhagic fever. *Antiviral Research* **64**, 145-160,  
973 doi:10.1016/J.ANTIVIRAL.2004.08.001 (2004).
- 974 29 Estrada, D. F. & De Guzman, R. N. Structural characterization of the Crimean-Congo hemorrhagic  
975 fever virus Gn tail provides insight into virus assembly. *The Journal of biological chemistry* **286**,  
976 21678-21686, doi:10.1074/jbc.M110.216515 (2011).
- 977 30 Freitas, N. *et al.* The interplays between Crimean-Congo hemorrhagic fever virus (CCHFV) M  
978 segment-encoded accessory proteins and structural proteins promote virus assembly and  
979 infectivity. *PLoS pathogens* **16**, e1008850-e1008850, doi:10.1371/journal.ppat.1008850 (2020).
- 980 31 Garrison, A. R. *et al.* A DNA vaccine for Crimean-Congo hemorrhagic fever protects against  
981 disease and death in two lethal mouse models. *PLOS Neglected Tropical Diseases* **11**, e0005908-  
982 e0005908 (2017).
- 983 32 Kortekaas, J. *et al.* Crimean-Congo Hemorrhagic Fever Virus Subunit Vaccines Induce High Levels  
984 of Neutralizing Antibodies But No Protection in STAT1 Knockout Mice. *Vector borne and zoonotic*  
985 *diseases (Larchmont, N.Y.)* **15**, 759-764, doi:10.1089/vbz.2015.1855 (2015).
- 986 33 Bertolotti-ciarlet, A. *et al.* Cellular Localization and Antigenic Characterization of Crimean-Congo  
987 Hemorrhagic Fever Virus Glycoproteins. *Society* **79**, 6152-6161, doi:10.1128/JVI.79.10.6152  
988 (2005).

989 34 Golden, J. W. *et al.* GP38-targeting monoclonal antibodies protect adult mice against lethal  
990 Crimean-Congo hemorrhagic fever virus infection. *Science Advances* **5**, eaaw9535-eaaw9535,  
991 doi:10.1126/sciadv.aaw9535 (2019).

992 35 McGettigan, J. P. *et al.* Second-Generation Rabies Virus-Based Vaccine Vectors Expressing  
993 Human Immunodeficiency Virus Type 1 Gag Have Greatly Reduced Pathogenicity but Are Highly  
994 Immunogenic. *Journal of Virology* **77**, 237 LP-244, doi:10.1128/JVI.77.1.237-244.2003 (2003).

995 36 Schnell, M. J., Buonocore, L., Whitt, M. A. & Rose, J. K. The minimal conserved transcription  
996 stop-start signal promotes stable expression of a foreign gene in vesicular stomatitis virus.  
997 *Journal of virology* **70**, 2318-2323, doi:10.1128/JVI.70.4.2318-2323.1996 (1996).

998 37 Smith, M. E. *et al.* Rabies virus glycoprotein as a carrier for anthrax protective antigen. *Virology*  
999 **353**, 344-356, doi:10.1016/j.virol.2006.05.010 (2006).

1000 38 Plummer, J. R. & McGettigan, J. P. Incorporating B cell activating factor (BAFF) into the  
1001 membrane of rabies virus (RABV) particles improves the speed and magnitude of vaccine-  
1002 induced antibody responses. *PLoS neglected tropical diseases* **13**, e0007800-e0007800,  
1003 doi:10.1371/journal.pntd.0007800 (2019).

1004 39 Wirblich, C. *et al.* One-Health: a Safe, Efficient, Dual-Use Vaccine for Humans and Animals  
1005 against Middle East Respiratory Syndrome Coronavirus and Rabies Virus. *Journal of virology* **91**,  
1006 e02040-02016, doi:10.1128/JVI.02040-16 (2017).

1007 40 Hudacek, A. W. *et al.* Recombinant rabies virus particles presenting botulinum neurotoxin  
1008 antigens elicit a protective humoral response in vivo. *Molecular Therapy - Methods & Clinical*  
1009 *Development* **1**, 14046-14046, doi:10.1038/mtm.2014.46 (2014).

1010 41 Sanchez, A. J., Vincent, M. J., Erickson, B. R. & Nichol, S. T. Crimean-Congo Hemorrhagic Fever  
1011 Virus Glycoprotein Precursor Is Cleaved by Furin-Like and SKI-1 Proteases To Generate a Novel  
1012 38-Kilodalton Glycoprotein. *Journal of Virology* **80**, 514 LP-525, doi:10.1128/JVI.80.1.514-  
1013 525.2006 (2006).

1014 42 Suda, Y. *et al.* Analysis of the entry mechanism of Crimean-Congo hemorrhagic fever virus, using  
1015 a vesicular stomatitis virus pseudotyping system. *Archives of Virology* **161**, 1447-1454,  
1016 doi:10.1007/s00705-016-2803-1 (2016).

1017 43 Vincent, M. J. *et al.* Crimean-Congo Hemorrhagic Fever Virus Glycoprotein Proteolytic Processing  
1018 by Subtilase SKI-1. *Journal of Virology* **77**, 8640 LP-8649, doi:10.1128/JVI.77.16.8640-8649.2003  
1019 (2003).

1020 44 Hernandez, A. *et al.* Phosphorylated Hexa-Acyl Disaccharides Augment Host Resistance Against  
1021 Common Nosocomial Pathogens. *Crit Care Med* **47**, e930-e938,  
1022 doi:10.1097/CCM.0000000000003967 (2019).

1023 45 Shao, S. *et al.* An Engineered Biomimetic MPER Peptide Vaccine Induces Weakly HIV Neutralizing  
1024 Antibodies in Mice. *Ann of Biomed Eng* **48**, 1991-2001, doi:10.1007/s10439-019-02398-8 (2020).

1025 46 Taleghani, N., Bozorg, A., Azimi, A. & Zamani, H. Immunogenicity of HPV and HBV vaccines:  
1026 adjuvanticity of synthetic analogs of monophosphoryl lipid A combined with aluminum  
1027 hydroxide. *APMIS* **127**, 150-157, doi:10.1111/apm.12927 (2019).

1028 47 Shearer, M. H., Dark, R. D., Chodosh, J. & Kennedy, R. C. Comparison and Characterization of  
1029 Immunoglobulin G Subclasses among Primate Species. *Clinical and Vaccine Immunology* **6**, 953-  
1030 958, doi:<https://doi.org/10.1128/CDLI.6.6.953-958.1999> (1999).

1031 48 Spellberg, B. & Edwards, J. E., Jr. Type 1/Type 2 Immunity in Infectious Diseases. *Clinical*  
1032 *Infectious Diseases* **32**, 76-102, doi:10.1086/317537 (2001).

1033 49 Iijima, N., Mattei, L. M. & Iwasaki, A. Recruited inflammatory monocytes stimulate antiviral Th1  
1034 immunity in infected tissue. *PNAS* **108**, 284-289, doi:<https://doi.org/10.1073/pnas.1005201108>  
1035 (2010).

1036 50 Blaney, J. E. *et al.* Antibody Quality and Protection from Lethal Ebola Virus Challenge in  
1037 Nonhuman Primates Immunized with Rabies Virus Based Bivalent Vaccine. *PLOS Pathogens* **9**,  
1038 e1003389-e1003389 (2013).

1039 51 Martin, R. M., Brady, J. L. & Lew, A. M. The need for IgG2c specific antiserum when isotyping  
1040 antibodies from C57BL/6 and NOD mice. *Journal of Immunological Methods* **212**, 187-192,  
1041 doi:[https://doi.org/10.1016/S0022-1759\(98\)00015-5](https://doi.org/10.1016/S0022-1759(98)00015-5) (1998).

1042 52 Johnson, N., Cunningham, A. F. & Fooks, A. R. The immune response to rabies virus infection and  
1043 vaccination. *Vaccine* **28**, 3896-3901, doi:<https://doi.org/10.1016/j.vaccine.2010.03.039> (2010).

1044 53 Hulswit, R. J. G., Paesen, G. C., Bowden, T. A. & Shi, X. Recent Advances in Bunyavirus  
1045 Glycoprotein Research: Precursor Processing, Receptor Binding and Structure. *Viruses* **13**, 353,  
1046 doi:10.3390/v13020353 (2021).

1047 54 Sahib, M. M. *Rapid Development of Optimized Recombinant Adenoviral Vaccines for  
1048 Biosafety Level 4 Viruses* Master of Science thesis, University of Manitoba, (2010).

1049 55 Fischinger, S., Boudreau, C. M., Butler, A. L., Streeck, H. & Alter, G. Sex differences in vaccine-  
1050 induced humoral immunity. *Semin Immunopathol* **41**, 239-249, doi:10.1007/s00281-018-0726-5  
1051 (2019).

1052 56 Dowall, S. D. *et al.* Protective effects of a Modified Vaccinia Ankara-based vaccine candidate  
1053 against Crimean-Congo Haemorrhagic Fever virus require both cellular and humoral responses.  
1054 *PLOS ONE* **11**, e0156637-e0156637 (2016).

1055 57 Haddock, E. *et al.* A cynomolgus macaque model for Crimean-Congo haemorrhagic fever. *Nature  
1056 microbiology* **3**, 556-562, doi:10.1038/s41564-018-0141-7 (2018).

1057 58 Harty, R. N., Brown, M. E., Hayes, F. P., Wright, N. T. & Schnell, M. J. Vaccinia virus-free recovery  
1058 of vesicular stomatitis virus. *Journal of molecular microbiology and biotechnology* **3**, 513-517  
1059 (2001).

1060 59 Schnell, M. J., Mebatsion, T. & Conzelmann, K. K. Infectious rabies viruses from cloned cDNA.  
1061 *The EMBO journal* **13**, 4195-4203 (1994).

1062 60 Johnson, R. F. *et al.* An Inactivated Rabies Virus-Based Ebola Vaccine, FILORAB1, Adjuvanted  
1063 With Glucopyranosyl Lipid A in Stable Emulsion Confers Complete Protection in Nonhuman  
1064 Primate Challenge Models. *The Journal of infectious diseases* **214**, S342-S354,  
1065 doi:10.1093/infdis/jiw231 (2016).

1066 61 Pulmanusahakul, R., Li, J., Schnell, M. J. & Dietzschold, B. The Glycoprotein and the Matrix  
1067 Protein of Rabies Virus Affect Pathogenicity by Regulating Viral Replication and Facilitating Cell-  
1068 to-Cell Spread. *Journal of Virology* **82**, 2330 LP-2338, doi:10.1128/JVI.02327-07 (2008).

1069 62 Burleson, F. G., Chambers, T. M. & Wiedbrauk, D. L. (eds Florence G. Burleson, Thomas M.  
1070 Chambers, & Danny L. B. T. *Virology* Wiedbrauk) 74-84 (Academic Press, 1992).

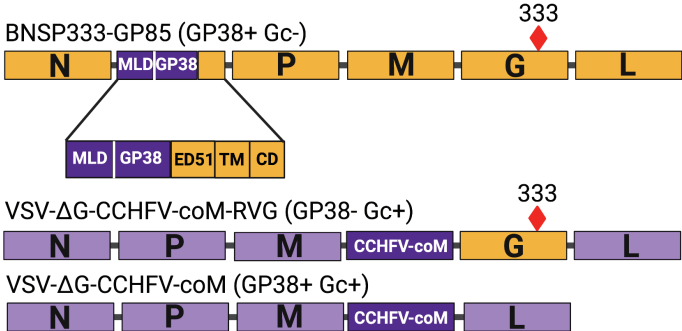
1071 63 Blaney, J. E. *et al.* Inactivated or Live-Attenuated Bivalent Vaccines That Confer Protection  
1072 against Rabies and Ebola Viruses. *Journal of Virology* **85**, 10605-10616, doi:10.1128/jvi.00558-11  
1073 (2011).

1074 64 Xia, H. *et al.* Transstadial Transmission and Long-term Association of Crimean-Congo  
1075 Hemorrhagic Fever Virus in Ticks Shapes Genome Plasticity. *Scientific reports* **6**, 35819-35819,  
1076 doi:10.1038/srep35819 (2016).

1077 65 Smith, J. S., Yager, P. A. & Baer, G. M. A rapid reproducible test for determining rabies  
1078 neutralizing antibody. *Bulletin of the World Health Organization* **48**, 535-541 (1973).

1079

**CCHFV Vaccines**



**Vector Controls**

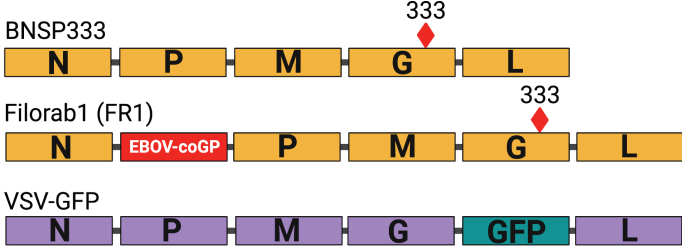


Figure 1



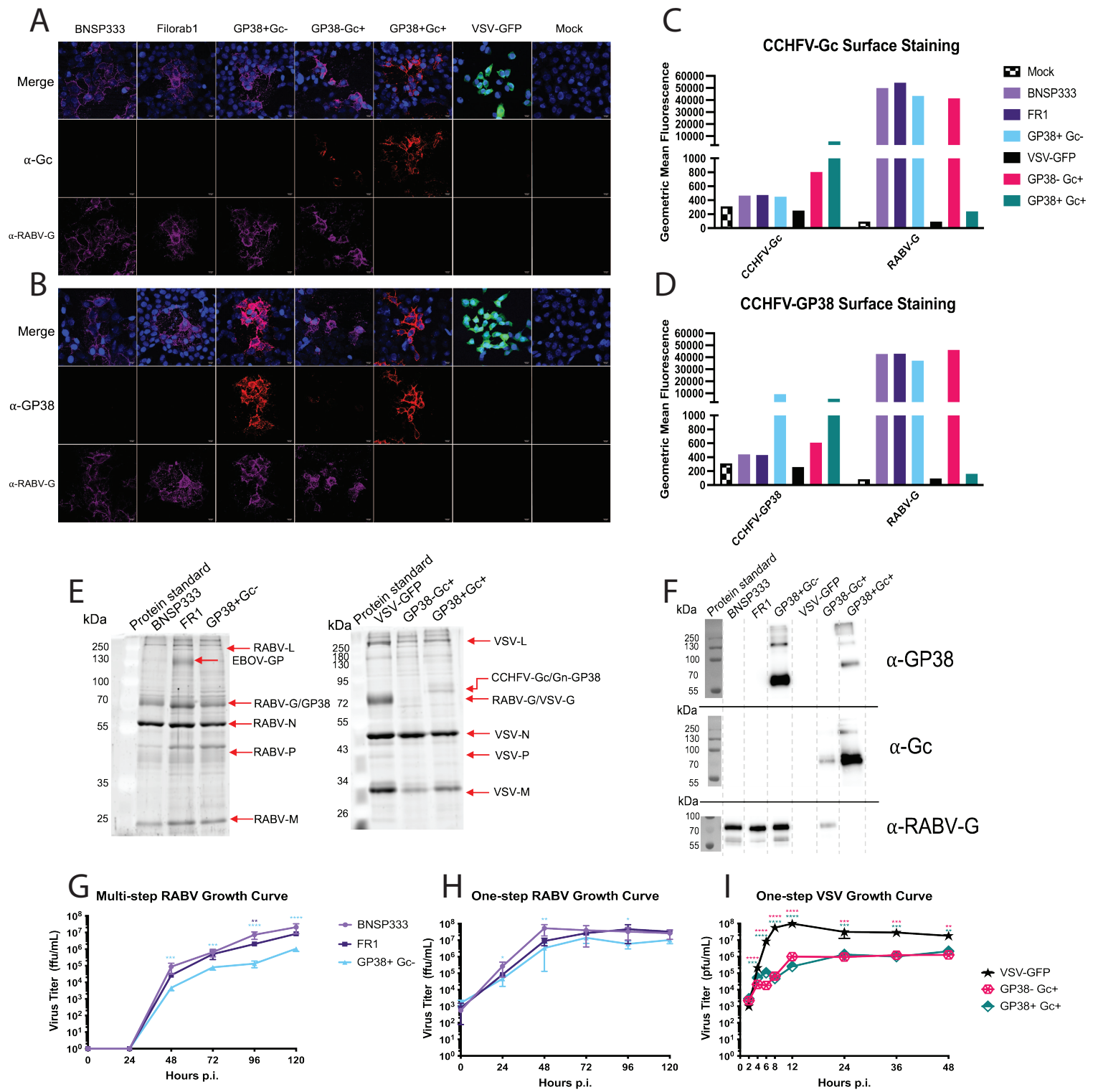


Figure 2

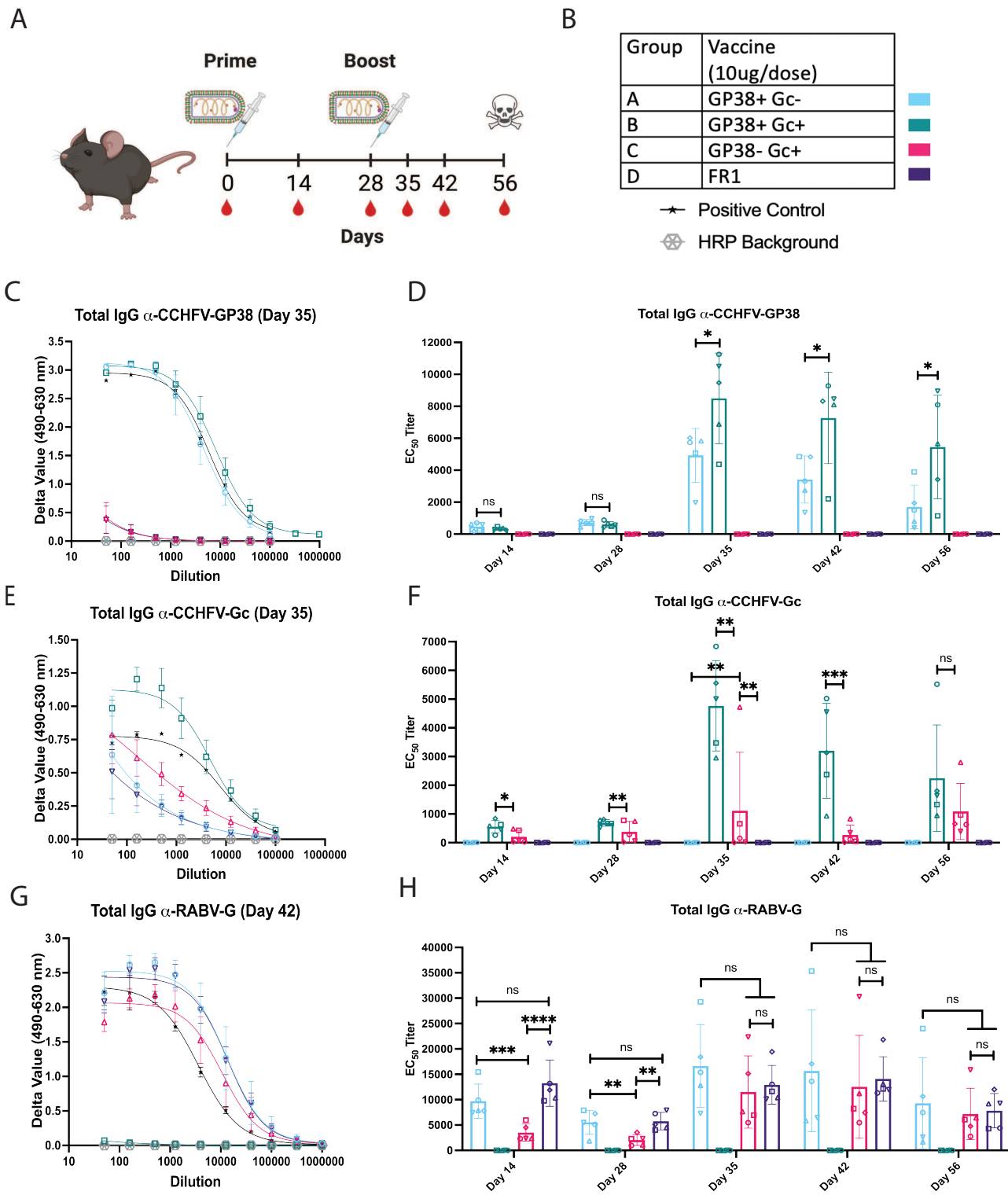


Figure 3

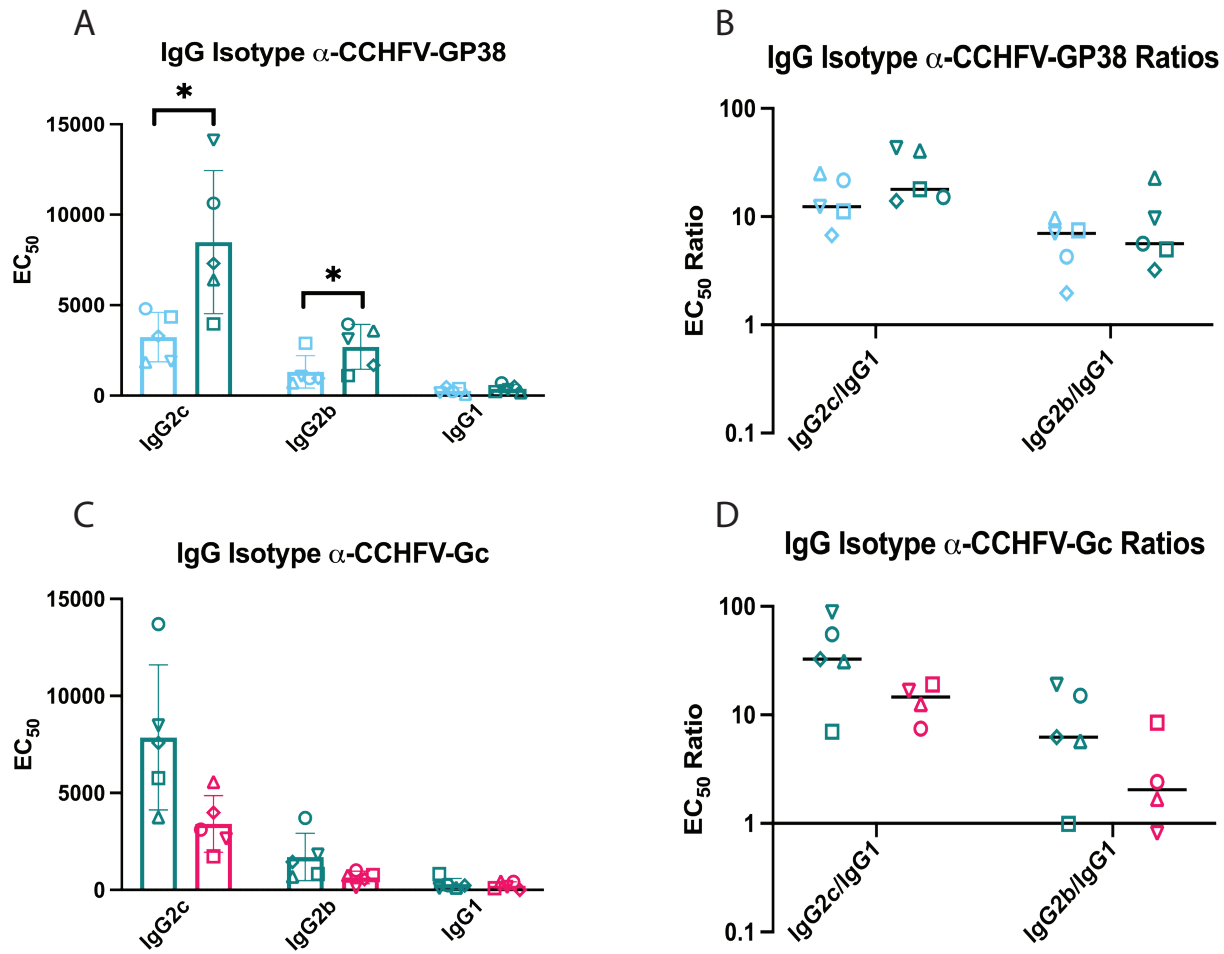


Figure 4

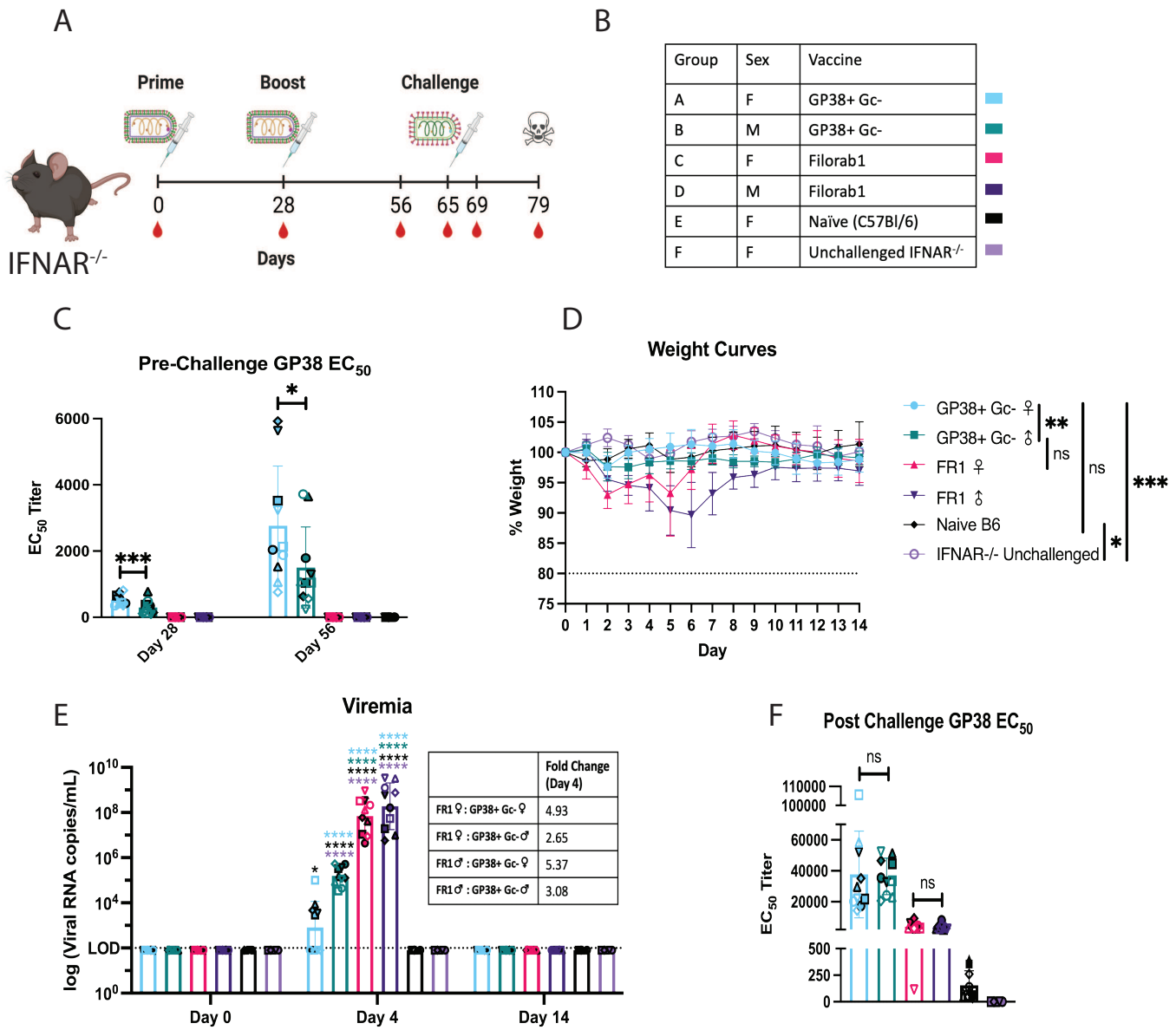


Figure 5

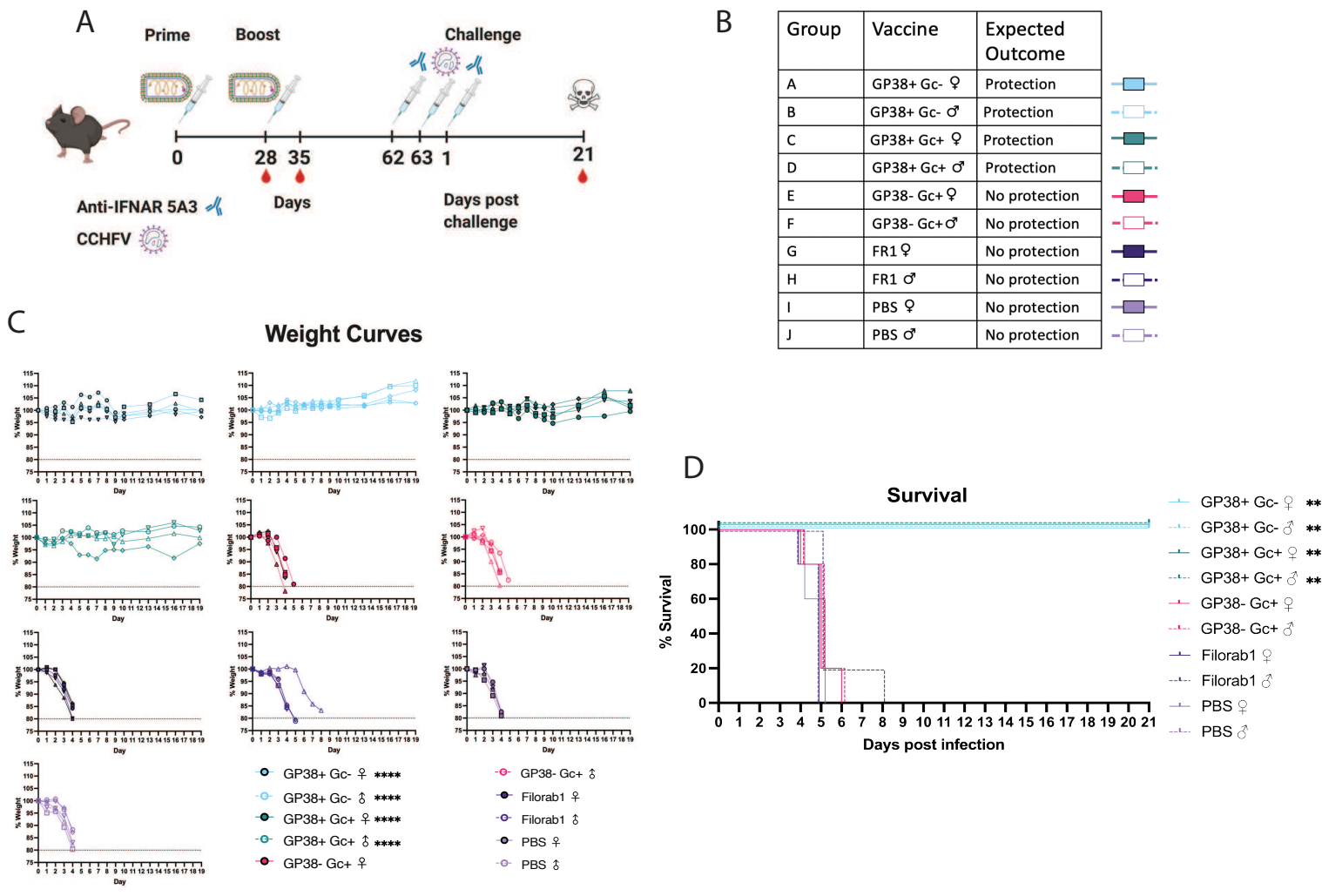


Figure 6

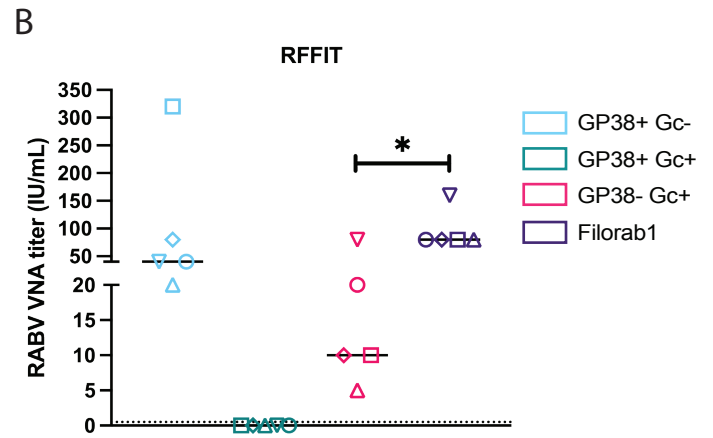
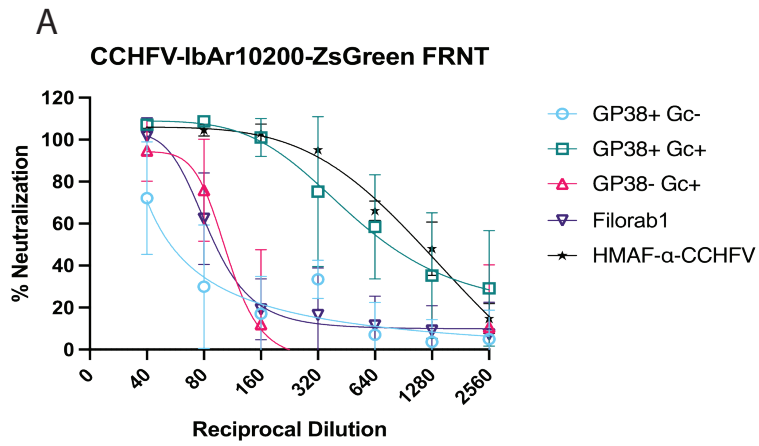
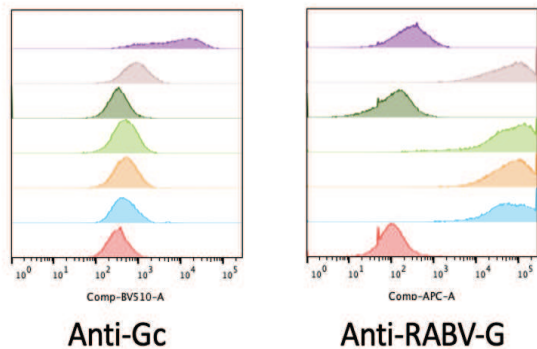


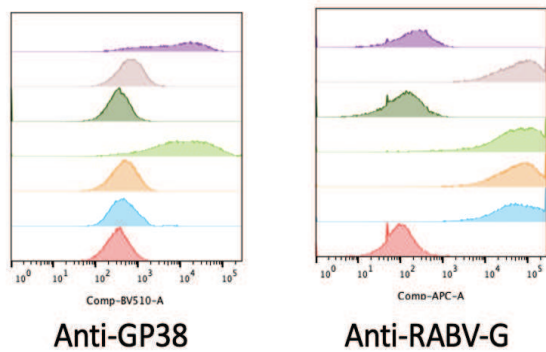
Figure 7

A



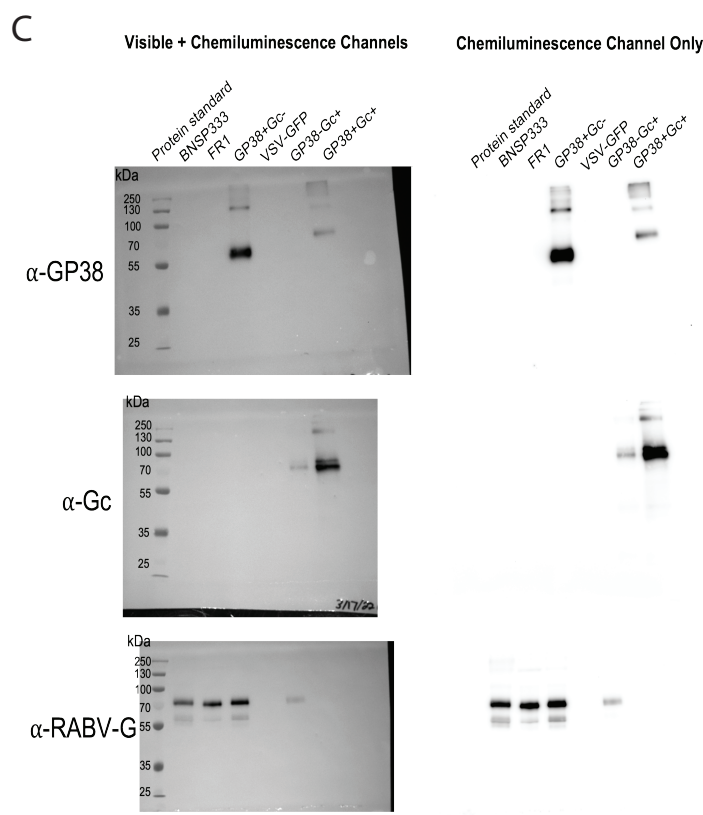
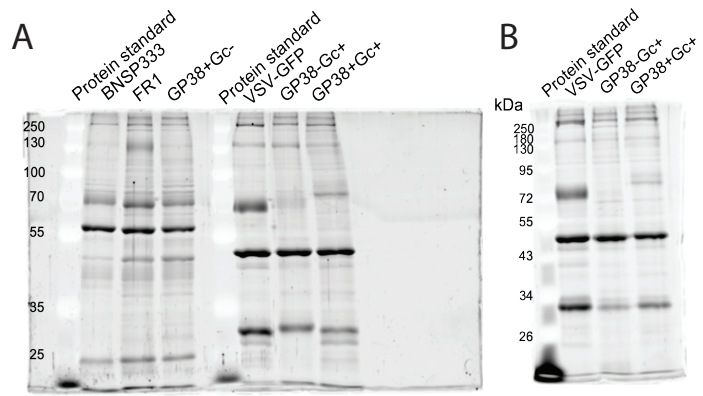
	Sample	Geometric Mean $\alpha$ -Gc	Geometric Mean $\alpha$ -RABV-G
	GP38+ Gc+	5607	241
	GP38- Gc+	807	41379
	VSV-GFP	253	93.6
	GP38+ Gc-	450	43554
	FR1	476	54374
	BNSP333	467	50060
	Mock	312	95.5

B



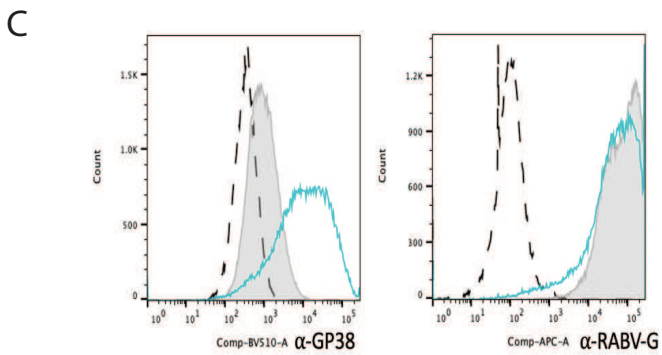
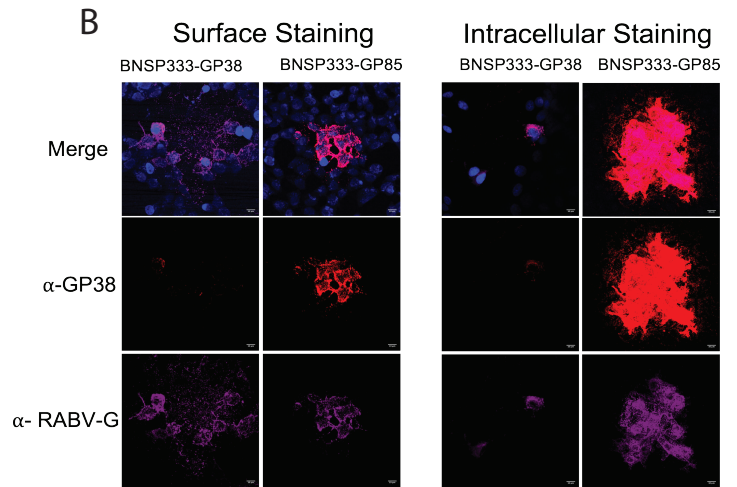
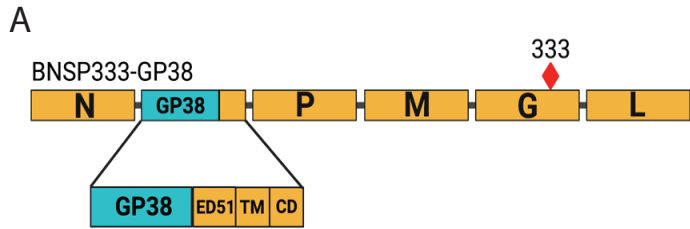
	Sample	Geometric Mean $\alpha$ -GP38	Geometric Mean $\alpha$ -RABV-G
	GP38+ Gc+	5494	163
	GP38- Gc+	610	46231
	VSV-GFP	259	96.1
	GP38+ Gc-	8456	34397
	FR1	433	42987
	BNSP333	442	42845
	Mock	313	86

Supplemental Figure 1

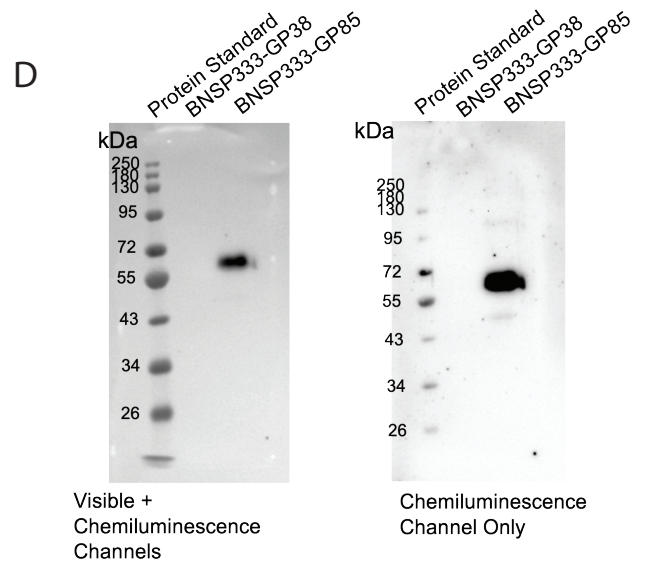


Supplemental Figure 2

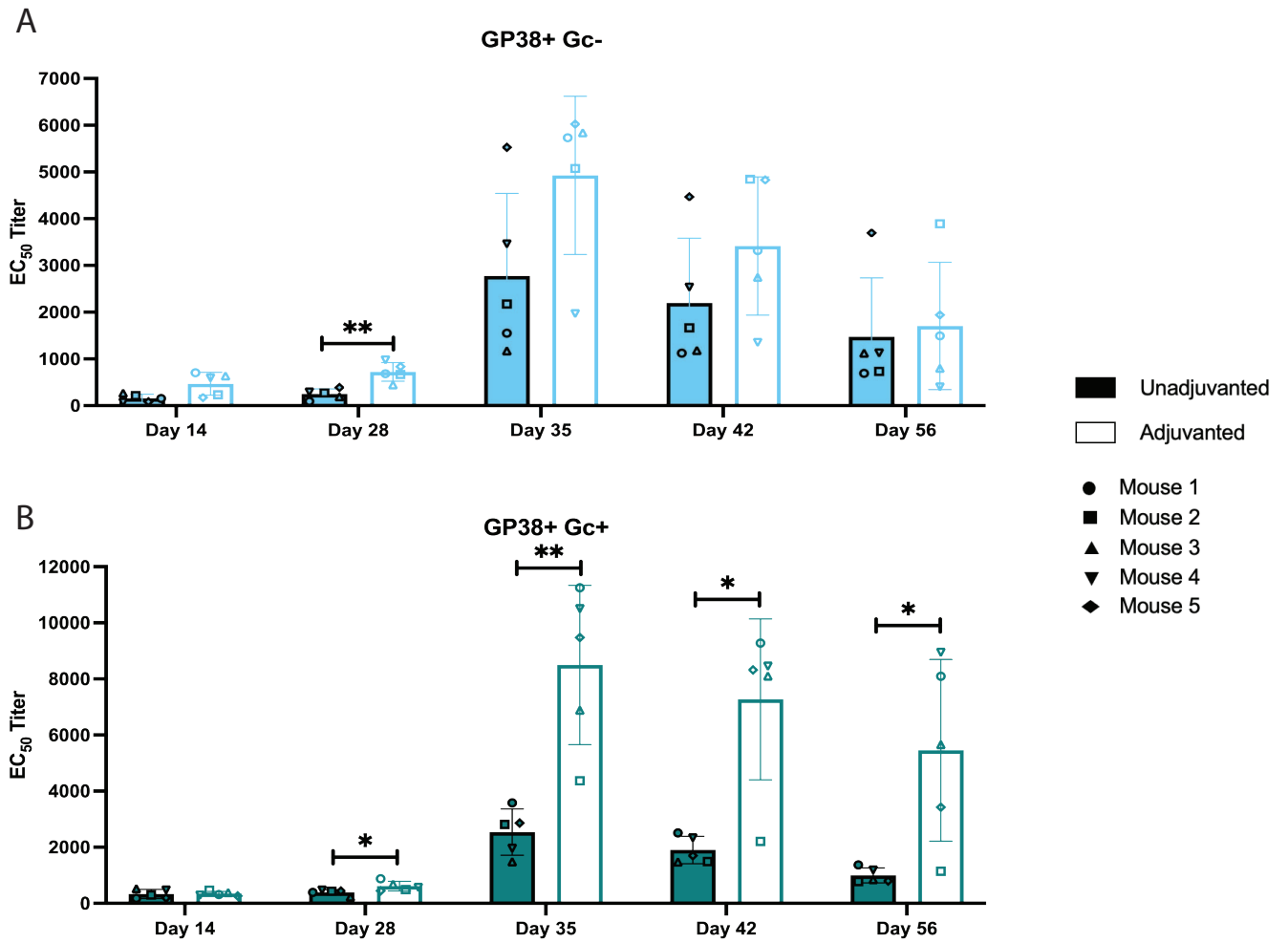




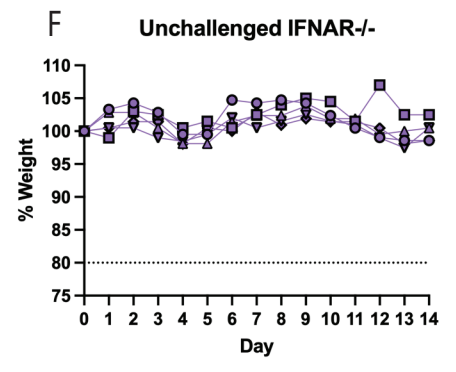
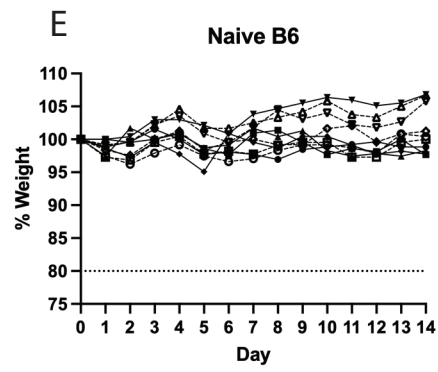
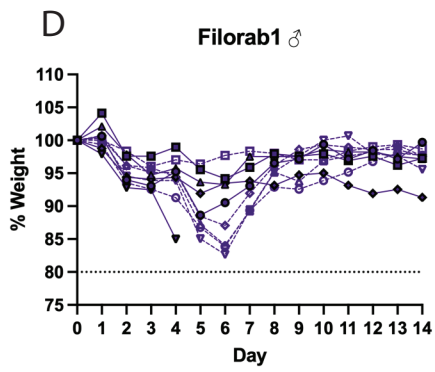
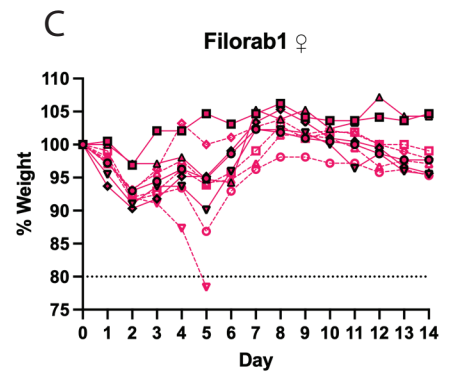
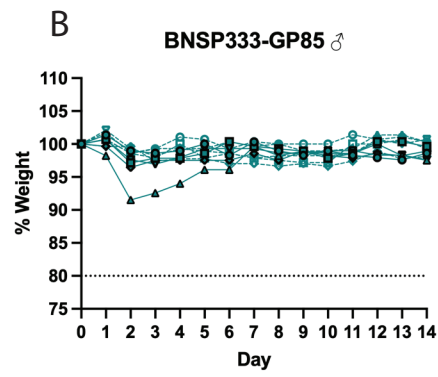
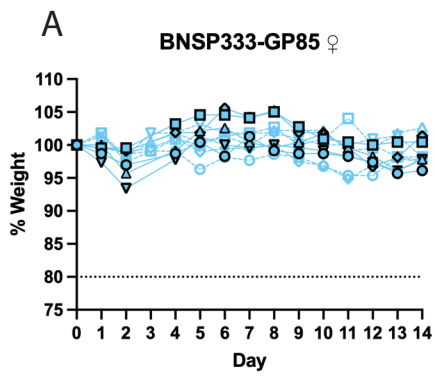
	Sample	Geometric Mean $\alpha$ -GP38	Geometric Mean $\alpha$ -RABV-G
	Mock	313	86
	BNSP333-GP38	869	63113
	BNSP333-GP85	8456	34397



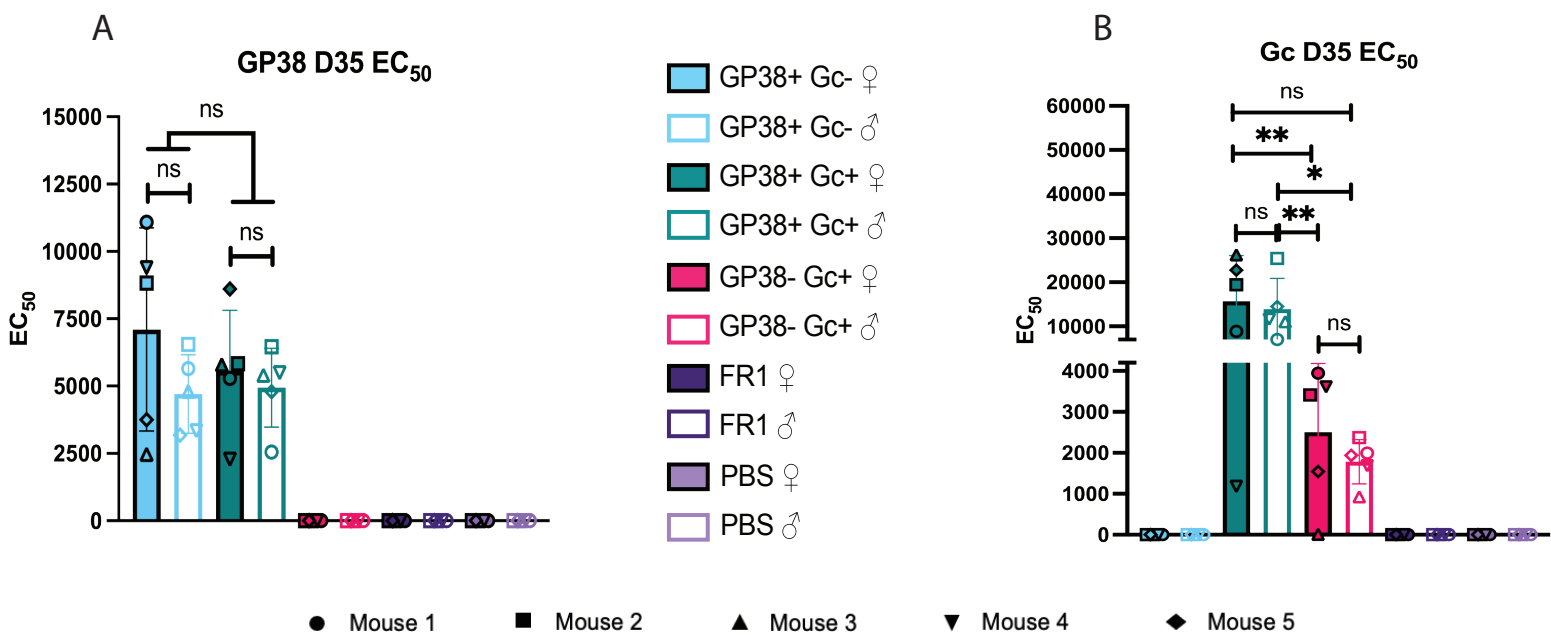
Supplemental Figure 3



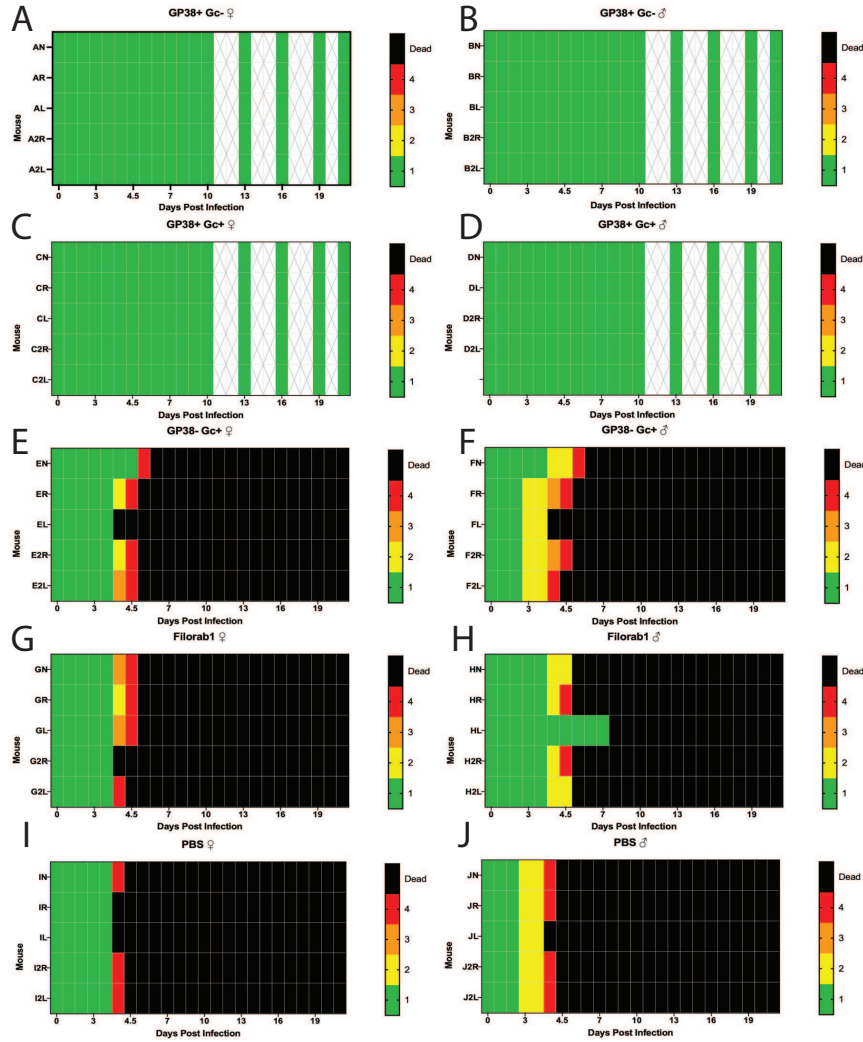
Supplemental Figure 4



Supplemental Figure 5



Supplemental Figure 6



Clinical Scoring Criteria	
1	Healthy
2	Ruffled fur, lethargic (triggers 2nd observation)
3	Ruffled fur, lethargic, hunched posture, orbital tightening (Triggers 3rd observation)
4	Reluctance to move when stimulated, paralysis, unable to access feed or water normally, moribund appearance, OR ≥20% weight loss -- Immediate euthanasia --

Supplemental Figure 7